

**EVALUATING THE EFFECTS OF DENSITY, VISCOSITY
AND SURFACE TENSION ON TWO-PHASE FLOW IN
HORIZONTAL PIPES**

BY

ALA SHAFEQ ABDULLAH AL-DOGAIL

**A Thesis Presented to the
DEANSHIP OF GRADUATE STUDIES**

**KING FAHD UNIVERSITY OF PETROLEUM & MINERALS
DHAHRAN, SAUDI ARABIA**

**In Partial Fulfillment of the
Requirements for the Degree of**

MASTER OF SCIENCE

In

PETROLEUM ENGINEERING

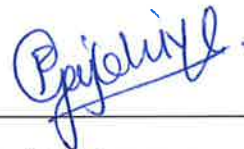
May 2018

KING FAHD UNIVERSITY OF PETROLEUM & MINERALS

DHAHRAN- 31261, SAUDI ARABIA

DEANSHIP OF GRADUATE STUDIES

This thesis, written by **ALA SHAFEQ ABDULLAH AL-DOGAIL** under the direction of his thesis advisor and approved by his thesis committee, has been presented and accepted by the Dean of Graduate Studies, in partial fulfillment of the requirements for the degree of **MASTER OF SCIENCE IN PETROLEUM ENGINEERING**.



Dr. Rahul Gajbhiye
(Advisor)



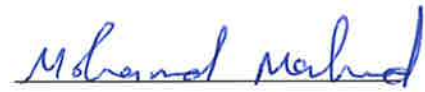
Dr. Dhafer AL-Shehri
Department Chairman



Dr. Salam A. Zummo
Dean of Graduate Studies



Date



Dr. Mohamed Mahmoud
(Member)



Dr. Salaheldin Elkatatny
(Member)



©Ala Shafeq Abdullah AL-Dogail

2018

DEDICATION

This thesis is dedicated to

MY BELOVED MOTHER & FATHER,

MY WIFE, MY DAUGHTER (NOOR), MY BROTHERS & SISTERS,

ALL MY FAMILY

ACKNOWLEDGMENTS

In the name of Allah, Most Gracious, Most Merciful. All praise is to Almighty Allah who gave me courage, knowledge, and ability to complete this work and blessing of Allah peace be upon his prophet Mohammed.

I really appreciate with great thanks and gratitude Dr. Rahul Gajbhiye, thesis advisor, Dr. Mohamed Mahmoud and Dr. Salaheldin Elkatatny, thesis committee members for providing their invaluable help and guidance through my thesis work.

Acknowledgment is due for King Fahd University of Petroleum & Minerals to give me a chance to complete my master degree. My sincere appreciation is extended to all faculty and staff of Petroleum Engineering Department for the contribution to this work. I would like to thank Mr. Abdulrahim Muhammadain, Mr. Abdul-Summed Iddrisu, Mr. Mobeen Murtaza for their priceless helping in PETE Departments laboratories.

Special thanks are due for all my colleagues and friends who help me in my work. Finally, I am indebted to Eng. A. A. Bugshan & HEFHD for their extreme moral support throughout my master program career and also for their encouragement.

TABLE OF CONTENTS

ACKNOWLEDGMENTS	V
TABLE OF CONTENTS.....	VI
LIST OF TABLES.....	VIII
LIST OF FIGURES.....	IX
LIST OF ABBREVIATIONS.....	XI
ABSTRACT	XII
ملخص الرسالة	XV
CHAPTER 1 INTRODUCTION.....	1
CHAPTER 2 LITERATURE REVIEW	3
2.1 Definition of Multi-Phase Flow in Horizontal Pipes.....	3
2.2 Classification of Flow Patterns in Horizontal Flow for Gas/Liquid System	3
2.3 Horizontal Flow	6
2.4 Previous Work.....	7
CHAPTER 3 METHODOLOGY.....	23
3.1 Experiment Description	23
3.1.1 Flow Loop Set-up	23
3.1.2 Preliminary Measurements	24
3.1.3 Experiment Procedure	28
3.2 Data Analysis.....	29
CHAPTER 4 RESULTS AND DISCUSSION.....	30

4.1 Flow Regime Results.....	30
4.1.1 Base Case (Air-Water) System	30
4.1.2 Effect of Surface Tension (σ).....	32
4.1.3 Effect of Viscosity (μ)	38
4.1.4 Effect of Density (ρ)	44
4.2 Pressure Drop Results	47
 CHAPTER 5 CONCLUSIONS AND RECOMMENDATIONS	 53
 REFERENCES.....	 55
 VITAE.....	 58

LIST OF TABLES

Table 2.1 Classification of Flow Regimes	5
Table 3.1 Surface Tension, Viscosity and Density Measurements of Different Surfactant Concentrations	25
Table 3.2 Viscosity, Surface tension and Density Measurements of Different Surfactant Concentrations	27
Table 3.3 Density, Surface tension and Viscosity Measurements of Different (CaBr ₂ with Surfactant) Concentrations	27
Table 3.4 Flowing Parameters	29

LIST OF FIGURES

Figure 2.1 Flow Pattern Categories	4
Figure 2.2 Transitional Sequence of Different Flow Regime Patterns Adapted from Reference[5].....	6
Figure 2.3 Baker’s Horizontal Pipes Flow Regime Map Adapted from Reference [10]....	9
Figure 2.4 Modified Baker’s Flow Pattern Map for Different Sizes Horizontal Pipelines Adapted from Reference[11].....	10
Figure 2.5 Modified Baker’s Flow Regime Map for Horizontal Pipelines Adapted from Reference [14]	11
Figure 2.6 Modified Baker’s Flow Regime Map for Horizontal Pipelines Adapted from Reference [15].....	12
Figure 2.7 Mandhane Horizontal Flow Pattern Map[17]	13
Figure 2.8 Taitel and Dukler’s Flow Regime Map for Horizontal Pipe[18]	14
Figure 2.9 Horizontal Flow Pattern Map[19]	16
Figure 2.10 Flow Pattern Map[3].....	17
Figure 2.11 Comparison Between Two Flow Pattern Maps, one is introduced by Lin and Hanratty [23] and Other Suggested by Mandhane et al.[17]	18
Figure 3.1 Horizontal Flow Loop	23
Figure 3.2 A Schematic of the Horizontal Flow Loop.....	24
Figure 3.3 Surfactant Concentrations (Vol %) versus Surface Tension (mN/m)	26
Figure 4.1 Flow Pattern Map of the Base Case (Air-Water)	31
Figure 4.2 Effect of Gas Superficial Velocity of the Base case (Air-Water, $V_{SL} = 2.67$ ft/sec).....	32
Figure 4.3 Flow Pattern Map of the (Air-0.02 Vol % Surfactant Concentration)	33
Figure 4.4 Effect of Gas Superficial Velocity of the (Air-0.02 Vol % Surfactant Concentration, $V_{SL} = 2.67$ ft/sec).....	33
Figure 4.5 Flow Pattern Map of the (Air-0.05 Vol % Surfactant Concentration)	34
Figure 4.6 Effect of Gas Superficial Velocity of the (Air-0.05 Vol % Surfactant Concentration, $V_{SL} = 2.67$ ft/sec).....	35
Figure 4.7 Flow Pattern Map of the (Air-0.1 Vol % Surfactant Concentration)	36
Figure 4.8 Effect of the gas superficial velocity of the (Air-0.1 Vol % Surfactant Concentration, $V_{SL} = 2.67$ ft/sec).....	36
Figure 4.9 Flow Pattern Map of the (Air-0.5 Vol % Surfactant Concentration)	37
Figure 4.10 Effect of Gas Superficial Velocity of the (Air-0.5 Vol % Surfactant Concentration, $V_{SL} = 2.67$ ft/sec).....	38
Figure 4.11 Flow Pattern Map of the (Air- 5 Vol % Glycerin Concentration).....	39
Figure 4.12 Effect of Gas Superficial Velocity of the (Air- 5 Vol % Glycerin Concentration, $V_{SL} = 2.67$ ft/sec).....	39

Figure 4.13 Flow Pattern Map of the (Air- 10 Vol % Glycerin Concentration).....	40
Figure 4.14 Effect of Gas Superficial Velocity of the (Air- 10 Vol % Glycerin Concentration, $V_{SL} = 2.67$ ft/sec).....	41
Figure 4.15 Flow Pattern Map of the (Air- 20 Vol % Glycerin Concentration).....	42
Figure 4.16 Effect of Gas Superficial Velocity of the (Air- 20 Vol % Glycerin Concentration, $V_{SL} = 2.67$ ft/sec).....	42
Figure 4.17 Flow Pattern Map of the (Air- 30 Vol % Glycerin Concentration).....	43
Figure 4.18 Effect of Gas Superficial Velocity of the (Air- 30 Vol % Glycerin Concentration, $V_{SL} = 2.67$ ft/sec).....	44
Figure 4.19 Flow Pattern Map of the (Air- 25 Vol% CaBr ₂ -0.004 Vol % Surfactant Concentration).....	45
Figure 4.20 Effect of Gas Superficial Velocity of the (Air- 25 Vol % CaBr ₂ -0.004 Vol % Surfactant Concentration, $V_{SL} = 2.67$ ft/sec).....	45
Figure 4.21 Flow Pattern Map of the (Air- 75% Calcium Bromide-0.02% Surfactant Concentration).....	46
Figure 4.22 Effect of Gas Superficial Velocity of the (Air- 75% CaBr ₂ -0.02% Surfactant Concentration, $V_{SL} = 2.67$ ft/sec).....	47
Figure 4.23 Pressure Drop Map of Air-Water System	48
Figure 4.24 Pressure Drop Map of Air-0.05% Surfactant System	49
Figure 4.25 Pressure Drop Map of Air-30% Glycerin System	50
Figure 4.26 Pressure Drop Map of Air-25% CaBr ₂ -0.004% surfactant System	51
Figure 4.27 Pressure Drop Map of Air-75% CaBr ₂ -0.02% surfactant System	52

LIST OF ABBREVIATIONS

M_L	:	Liquid Mass Flow Rate (cu. ft/Min)
M_G	:	Gas Mass Flow Rate (cu. ft/Min)
V_{SL}	:	Liquid Superficial Velocity (ft/sec)
V_{SG}	:	Gas Superficial Velocity (ft/sec)
L	:	Liquid Mass Flux (lb/hft^2)
G	:	Gas Mass Flux (lb/hft^2)
VSD	:	Variable Speed Drive
ρ	:	Density (gm/cc)
σ	:	Surface Tension (mN/m)
μ	:	Viscosity (cP)

ABSTRACT

Full Name : [Ala Shafeq Abdullah AL-Dogail]
Thesis Title : [Evaluating the Effects of Density, Viscosity and Surface Tension on Two-Phase Flow in Horizontal Pipes]
Major Field : [Petroleum Engineering]
Date of Degree : [May, 2018]

Two-phase gas/liquid flow regime in pipes is a common occurrence in different applications. In oilfield facilities, two-phase flow can occur in different parts of production system such as flow of fluid through tubing and pipelines. During the design of a production system, accurate prediction of pressure drop is imperative which is determined from flow pattern and flow regime map. Unfortunately, most of the flow regime maps were developed without considering the effect of fluid properties (density, viscosity and surface tension). In spite of the practical importance, the general applicability of these maps is not addressed. In order to improve generality of flow regime maps it is necessary to evaluate the effect of density (density of water 62.4 lb/cu.ft and for oil 50 lb/cu.ft), viscosity (viscosity of water 1 centipoise and for oil 10 centipoises at standard conditions) and surface tension which differ by great magnitude (air/water = 72 mN/m and gas/oil = 35 mN/m) on flow regime map. Thus, this work aims to evaluate the effect of liquid density, liquid viscosity, and surface tension on the flow regime map and address its applications.

Several studies on two-phase flow through horizontal pipelines have been performed to develop the flow regime maps. As a result, many flow pattern maps have been

established. Such studies include those done by Baker, Govier & Aziz, Mandhane, Beggs & Brill, etc. Further, to formulate the flow regime maps, some mapping parameters and dimensionless groups are used as coordinates. Some of the parameters are liquid and gas superficial velocities, mass flux, gas-liquid properties (density, viscosity, etc.) and dimensionless numbers such as gas velocity number, liquid velocity number, Weber number, and Froude numbers. To generalize the applicability of the flow regime maps, a combination of parameters and dimensionless numbers are used.

To generate these maps lots of experimental data is required and usually, it is not feasible to evaluate the effect of each individual parameter (density, viscosity, surface tension, pipe size or geometry) on the flow regime map. Presence of interfaces between two different phases refers to the multi-phase flow. Surface tension is utilized to characterize the existence of an interphase and this effect was not evaluated for the air-water flow system despite the fact that most of the studies reported in the literature consider the air-water system to generate the experimental data required for flow regime map.

The purpose of this work is to evaluate the influence of density, viscosity and surface tension on flow regimes in horizontal pipe and investigate its effects on boundary transition. The experiments were conducted on a horizontal pipe flow-loop (length 30' and diameter 1") with two-phase air/liquid. The range of superficial gas velocity is 0-60ft/s and superficial liquid velocity is 0-10ft/s. The effect of density was introduced by increasing the density with aid of Calcium Bromide salt, the effect of viscosity was introduced by increasing the viscosity with aid of glycerin, and the effect of surface tension was introduced by reducing the surface tension with the aid of a surfactant. Two different Calcium Bromide concentrations (25 and 75%), four different glycerin

concentrations (5, 10, 20, 30%), and four different surfactant concentrations (0.02, 0.05, 0.1, 0.5%) were selected and the experimental data was utilized to generate flow pattern map and the effect of density, viscosity, and surface tension were evaluated based on the variation in the boundaries of different flow patterns.

ملخص الرسالة

الاسم الكامل: علاء شفيق عبدالله الدقيل

عنوان الرسالة: تقييم تأثير الكثافة واللزوجة والشد السطحي على الجريان ثنائي الطور في الأنابيب الأفقية

التخصص: هندسة بترول

تاريخ الدرجة العلمية: مايو 2018

أنماط الجريان ثنائي الطور للغاز والسائل شائع الحدوث في تطبيقات مختلفة. في منشآت الحقول النفطية، الجريان ثنائي الطور يمكن أن يحدث في حالات مختلفة والتي منها جريان الموائع داخل خطوط الأنابيب. أثناء التصميم لنظام الإنتاج، يتطلب التنبؤ الدقيق لإنخفاض الضغط والذي يتم تحديده من خرائط أنماط الجريان. ولكن لسوء الحظ فإن معظم خرائط أنماط الجريان تم تصميمها دون الأخذ بالإعتبار تأثير خصائص المائع (الكثافة واللزوجة والشد السطحي). بالرغم من الأهمية العملية لهذه الخرائط، فإن التطبيق العام لهذه الخرائط لم يعالج بعد. ولتحسين عمومية خرائط أنماط الجريان، من الضروري تقييم تأثير الكثافة (كثافة الماء 62.4 رطل لكل قدم مكعب وللنفط 50 رطل لكل قدم مكعب) واللزوجة (لزوجة الماء 1 سنتيبويس ولزوجة النفط 10 سنتيبويس عند الظروف الإعتيادية) والشد السطحي الذي يختلف بقيمه كبيرة (72 ملي نيوتن لكل متر للماء و 35 ملي نيوتن لكل متر للنفط) على خريطة أنماط الجريان. لذلك تهدف هذه الدراسة لتقييم تأثير الكثافة واللزوجة والشد السطحي على خريطة نمط الجريان ومعالجة تطبيقاتها. العديد من البحوث للجريان ثنائي الطور في خطوط الأنابيب تم عملها ونتيجة لذلك تم تصميم العديد من خرائط أنماط الجريان. بعض هذه الدراسات تضمنت الخرائط التي أنشئت بواسطة بيكر، قوفير وعزيز، مانهاني، بيقس وبيريل وغيرهم. علاوة على ذلك ولصياغة خرائط أنماط الجريان. بعض متغيرات الرسم والمجموعات التي لا بعد لها إستخدمت كمحاور. بعض المتغيرات هي السرعات السطحية للسائل والغاز وتدفق الكتلة وخصائص

المائع (الكثافة واللزوجة إلخ) والأرقام اللابعديّة مثل رقم سرعة السائل ورقم سرعة الغاز وعدد ويبر وعدد فريد. ولتعميم التطبيق لخرائط أنماط الجريان. مزيج من المتغيرات والأرقام اللابعديّة إستخدمت.

ولإنشاء هذه الخرائط الكثير من البيانات التجريبية مطلوبة وفي الغالب من غير الممكن تقييم تأثير كل متغير بمفرده (الكثافة واللزوجة والشد السطحي وحجم الانبوب والشكل الهندسي) على خريطة أنماط الجريان. الجريان متعدد الاطوار يتميز بوجود واجهات بين الاطوار وانقطاعات للخصائص المرافقة . الشد السطحي يستخدم ليميز وجود واجهة وهذا التأثير لم يقيم لنظام الهواء والماء بالرغم من حقيقة ان معظم الدراسات تأخذ في الاعتبار نظام الهواء والماء لتوليد البيانات التجريبية المطلوبة لخريطة نمط الجريان.

الغرض من هذه الدراسة هو تقييم تأثير الكثافة واللزوجة والشد السطحي على أنماط الجريان في الأنابيب الأفقية وتحقيق تأثيرها على إنتقال الحدود. تم عمل التجارب باستخدام أنبوب إفتي طوله 30 قدم وقطرة 1 بوصة لجريان ثنائي الطور للهواء والسائل . سرعة الغاز السطحية تتراوح ما بين (0 إلى 60 قدم لكل ثانية) بينما السرعة السطحية للسائل تتراوح ما بين (0 إلى 10 قدم لكل ثانية). تقييم تأثير الكثافة تم من خلال زيادة الكثافة بإستخدام ملح بروميد الكالسيوم ، تقييم تأثير اللزوجة تم من خلال زيادة اللزوجة بإستخدام الجلوسرين وتقييم تأثير الشد السطحي تم من خلال تقليل الشد السطحي بإستخدام التوتر السطحي . تم إستخدام تركيزين مختلفين (25 و75%) من ملح بروميد الكالسيوم ، أربع تراكيز مختلفة (5 و 10 و20 و30) من الجلوسرين وأربع تراكيز مختلفة من التوتر السطحي وتمت الإستفادة من البيانات التجريبية لإنشاء خرائط أنماط الجريان وتم تقييم تأثير الكثافة واللزوجة والشد السطحي من خلال الاختلافات في الحدود لمختلف أنماط الجريان.

CHAPTER 1

INTRODUCTION

Multi-phase flow is defined as simultaneous flow with different phases and it is a very common occurrence in nature and there are many examples of multi-phase flow in our environments such as rain, snow, fog, avalanches, mudslides, sediment transport and debris flow. Furthermore, Multi-phase flow occurs commonly in different industries such as petroleum, chemical, nuclear and geothermal industry. In the oil fields, gas-liquid flow occurs in oil producing wells and associated flow lines, separators, dehydration units, evaporators and other processing equipment. A mixture of fluid compounds flowing through a pipe can exit as a single-phase liquid, single-phase gas, or a two-phase gas-liquid mixture. However, the behavior of two-phase flow systems is more complex than that of single-phase schemes because of the phase distribution variations in the pipe. The variation and distribution of the phases have specific characteristics, these characteristics of flow known as the flow pattern or flow regime. There are many factors and forces acting on the fluids affect the types of flow patterns that exist at a certain location in the pipe. These flow parameters involve turbulence, buoyancy, inertia, and surface tension forces in addition to volume fluxes, pipe diameter, and deviation angle.

A good estimation of the multi-phase flow patterns will lead to a precise prediction of the pressure drop in the pipelines. In addition, the geometric distribution of the flowing components has sensitive effects on momentum, mass, and energy transfer rates and

processes. Also, flow patterns provide significant information for many associated flow problems such as erosion and corrosion prediction, and prediction of solids deposition and slug characteristics.

The flow patterns or flow regimes are terms used to recognize the geometric distribution of the flowing components in the pipes. The instability of the regimes causes the instability of the flow patterns boundaries in a flow regimes map and consequently, the transition to another flow pattern occurs. Usually visual inspection used to recognize the flow patterns, however, when visual information is difficult to obtain, the fluctuations in the volume fraction or the spectral content of the unsteady pressures have been devised [1]. Flow patterns are classified for interpreting the flow patterns resulted in a vast array of flow regime names. In case of the horizontal flow in pipelines, the flow regimes of air/water system are categorized into four main classes, stratified flow regime, intermittent flow regime, annular flow regime and dispersed bubble flow regime [2].

The aim of this work is to evaluate the influence of fluid viscosity, surface tension, and fluid density on the flow patterns in horizontal flow pipe. Surface tension effect was studied for different concentrations of surfactant which reduces the surface tension between air and water while fluid density and fluid viscosity are constant. Different concentrations of Calcium Bromide (CaBr_2) salt have been used to increase the density of the fluid and the effect of fluid density on flow regimes was evaluated by keeping surface tension and fluid viscosity constant. Different concentrations of glycerin, which increase the fluid viscosity, was used to study the impact of fluid viscosity on the flow regimes while surface tension and fluid density were constant.

CHAPTER 2

LITERATURE REVIEW

2.1 Definition of Multi-Phase Flow in Horizontal Pipes

Multi-phase flow in horizontal pipes is defined as the flow of different phases such as gas phase, solid phase, and liquid phase simultaneously through horizontal pipelines. Flow patterns or flow regimes are terms used to recognize the geometric distribution of the flowing components in the pipes and provide significant information for many associated flow problems such as prediction of scale erosion, chemical corrosion, asphaltene deposition, and slug characteristics. Accurate prediction of multi-phase flow regimes is necessary for pressure calculations to get a good estimation of pressure drop during fluid flow process.

2.2 Classification of Flow Patterns in Horizontal Flow for Gas/Liquid System

Two-phase flow system through pipelines is controlled with different parameters and the flow patterns are the most important parameter that should be considered during pressure drop calculation. Several researchers classified flow patterns for interpreting the flow patterns according to resulted in a vast array of flow regime names. Barnea (1987)[2] classified the flow regimes of air/water system in horizontal pipelines into four main categories as follows:

1-Stratified flow (i.e. smooth flow and wavy flow)

2- Intermittent flow (i.e. plug flow and slug flow)

3-Annular flow (i.e. misty flow and wavy flow)

4-Dispersed bubble flow

Figure 2.1 shows the main categories of horizontal flow patterns for air/water system

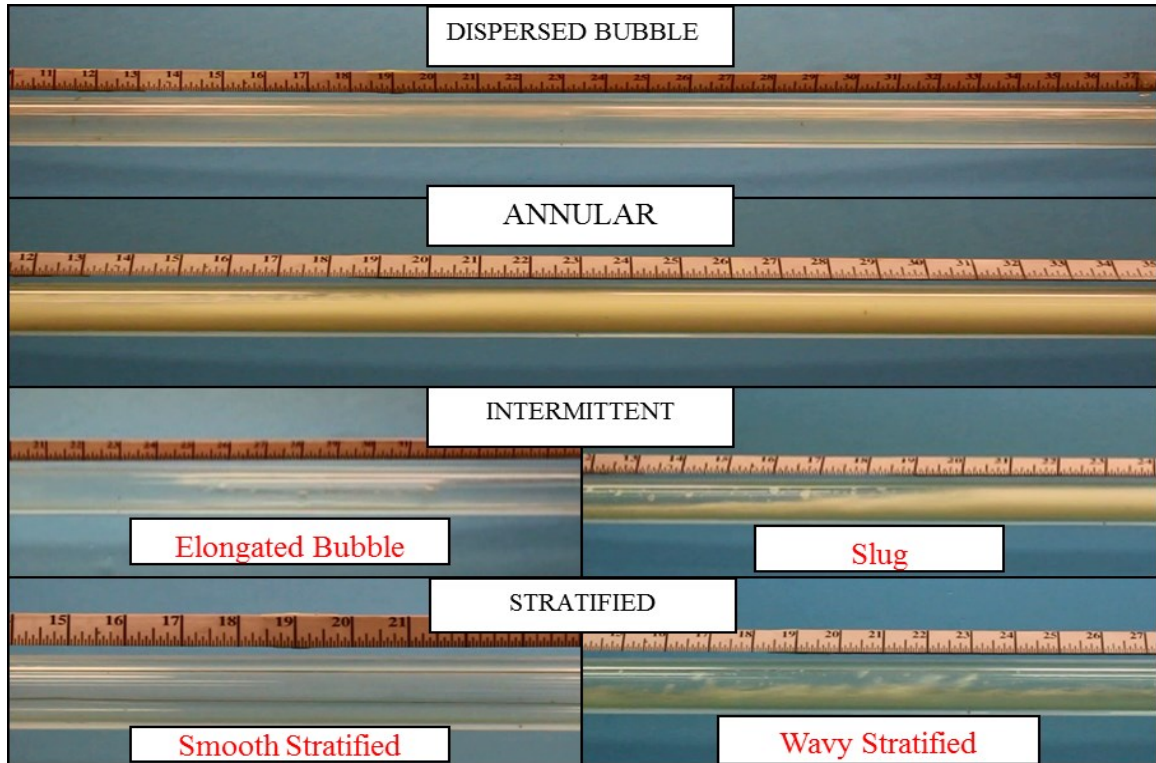


Figure 2.1 Flow Pattern Categories

Spedding and Nguyen (1979)[3], Kokal and Stanislav (1993)[4], Wong and Yau (1997)[5], and Barnea (1987)[2] classified the flow patterns into four main regimes depending on observations by videography. In the first category, both gas and liquid phases are flow separately from each other where gas phase rises above the liquid phase during flowing through horizontal pipelines. No droplets or bubbles can be formed during this flow regime and this flow is known as stratified flow. This category of flow can be subdivided into the stratified flow, stratified with ripple wave flow, stratified with roll wave and stratified with inertial wave flow. The second category of flow pattern is called

intermittent flow and it happens when the heavier phase (liquid) is continuous while lighter one (gas) is discontinuous. In case both gas and liquid phases are discontinuous, this is called mixed flow regime; whereas, a dispersed bubble happens when the heavier phase (liquid) is discontinuous and the lighter phase (gas) is continuous. These main flow regimes also subdivided into more detailed classification as shown in Table 2.1, while the transitional sequence of these flow patterns is illustrated in Figure 2.2.

Table 2.1 Classification of Flow Regimes

a) Stratified	b) Intermittent	c) Mixed flow	d) Dispersed bubble
1) Smooth 2) Inertial wave 3) Ripple wave 4) Roll wave	1) Plug 2) Slug 3) Plug-slug 4) Pseudo-slug	1) Roll wave + Droplet 2) Roll wave + Droplet + Annular 3) Roll wave + Annular 4) Pseudo-slug + Annular 5) Pseudo-slug + Thin annular 6) Slug + Annular 7) Dispersed bubbles + Slug	Dispersed bubbles

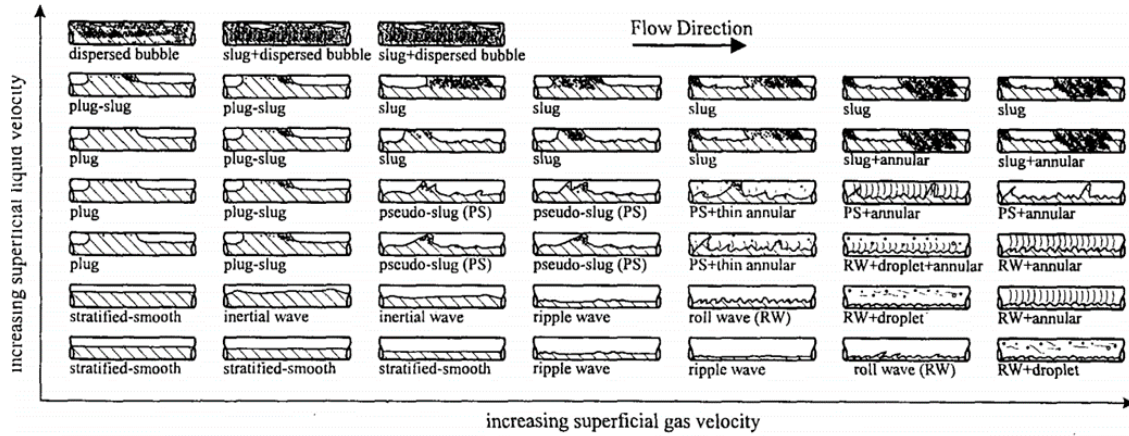


Figure 2.2 Transitional Sequence of Different Flow Regime Patterns Adapted from Reference[5]

There are several studies have been conducted to study the effect of: volume flux, volume fraction, viscosity, density and surface tension of components on flow regimes. The results of previous studies were presented in different figures called flow regime maps. Unfortunately, these regime maps have limitations where they can be used only with specific sizes of pipelines or specific fluids similar to fluids that tested by researchers. In other words, these regime maps don't give accurate results when they are applied to different pipe sizes or different fluids properties. Indeed, the several represented transitions of the most flow pattern maps have instabilities and they are controlled by numerous fluid properties.

2.3 Horizontal Flow

Many flow regime maps were developed for horizontal flow. Kosterin, in 1949, was the pioneer in this research and he was the first researcher to suggest the use of flow regime maps[6]. Since then, many researchers (1954 –1987) proposed many flow regime maps for identifying the general flow patterns for a two-phase flow system. Baker (1954) developed a common flow regime map for a two-phase system based on the experimental

data gathered from references [Jenkins (1947), Gazely (1948), Kosterh (1949) and Alves (1954)][6] and it is still widely used in petroleum industry.

2.4 Previous Work

Bergelin and Gazley (1949)[7] suggested flow pattern maps of the system consisting of air and water flowing through 1-inch pipe diameter. They used a mass flow rate of both liquid and gas phases, M_L and M_G , as map coordinates. Similar work was done by Johnson and Abou-Sabe (1952)[8] with a little difference in pipe diameter where 0.87 in pipe diameter was utilized in that experiments.

Alves (1954)[9] studied the flow of different mixtures, some of them consist of air-water while others consist of air-oil, in a 1-inch pipe diameter and he presented his results on a single map. Superficial velocity for liquid and gas, V_{SL} and V_{SG} was used in this study as the coordinates for the flow regime map.

Baker (1954)[10] studied two-phase flow through horizontal pipelines the flow regime map were developed based on the experimental data gathered from literature [Jenkins (1947), Gazely (1948), Kosterh (1949) and Alves (1954)]. Figure 2.3 shows the Baker's flow regime map where the X-axis and Y-axis were defined as follows:

$$\text{X-axis: } \frac{L \lambda \psi}{G}$$

$$\text{and Y-axis: } \frac{G}{\lambda} [\text{lb/h ft}^2]$$

where, L and G represent mass flux of both liquid and gas through pipe respectively and they can be calculated as the following:

$$L = \frac{m_L}{S} [lb/hft^2] \quad (1)$$

$$G = \frac{m_G}{S} [lb/hft^2] \quad (2)$$

The parameters λ and ψ in coordinates definition can be calculated as the following:

$$\lambda = \left[\frac{\rho_G}{\rho_{air}} \frac{\rho_L}{\rho_w} \right]^{1/2} \quad (3)$$

$$\Psi = \frac{\sigma_w}{\sigma_L} \left[\frac{\mu_L}{\mu_w} \left(\frac{\rho_w}{\rho_L} \right)^2 \right]^{1/3} \quad (4)$$

Densities of air and water in the above equations were measured at room conditions ($\rho_{air} = 0.075 \text{ lb/ft}^3$ and $\rho_w = 62.3 \text{ lb/ft}^3$). Surface tension for water also was measured at room conditions also ($\sigma_w = 73 \text{ dyn/cm}$). $\mu_w = 1 \text{ cp}$ is the water viscosity.

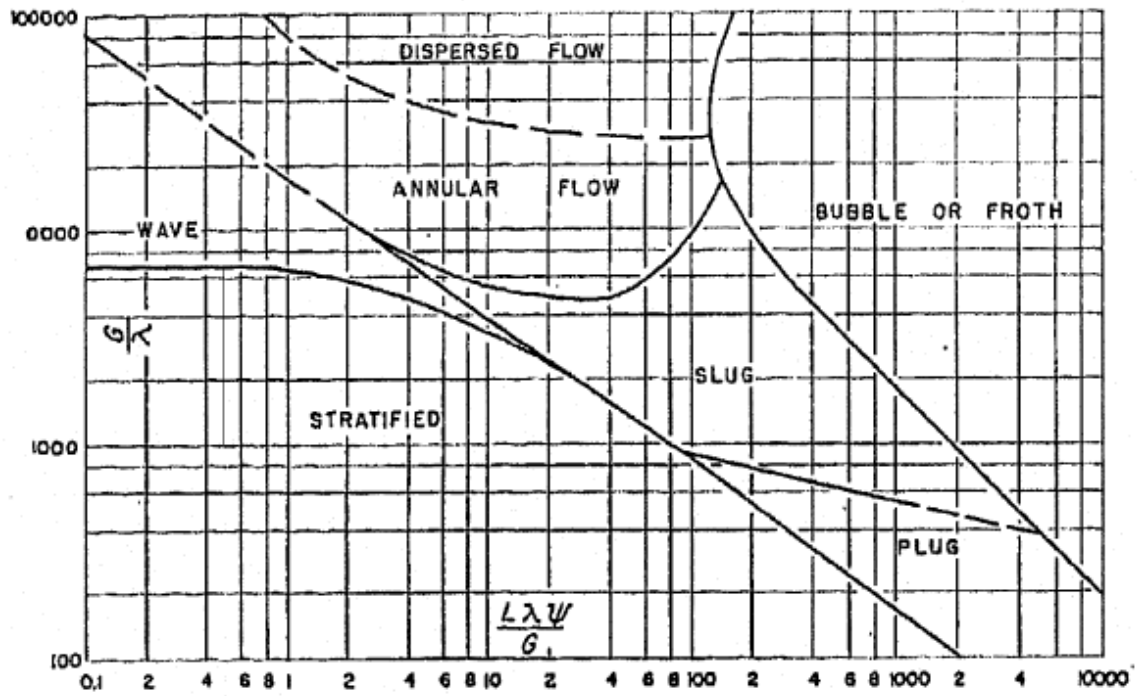


Figure 2.3 Baker's Horizontal Pipes Flow Regime Map Adapted from Reference [10]

Scott (1964) [11] tried to modify Baker's flow regime map by introducing the effect of pipe diameter in his study. The author used data gathered from different references [Hoogendoorn (1959)[12] and of Govier and Omer (1962)[13]] during modification of his work as presented in Figure 2.4.

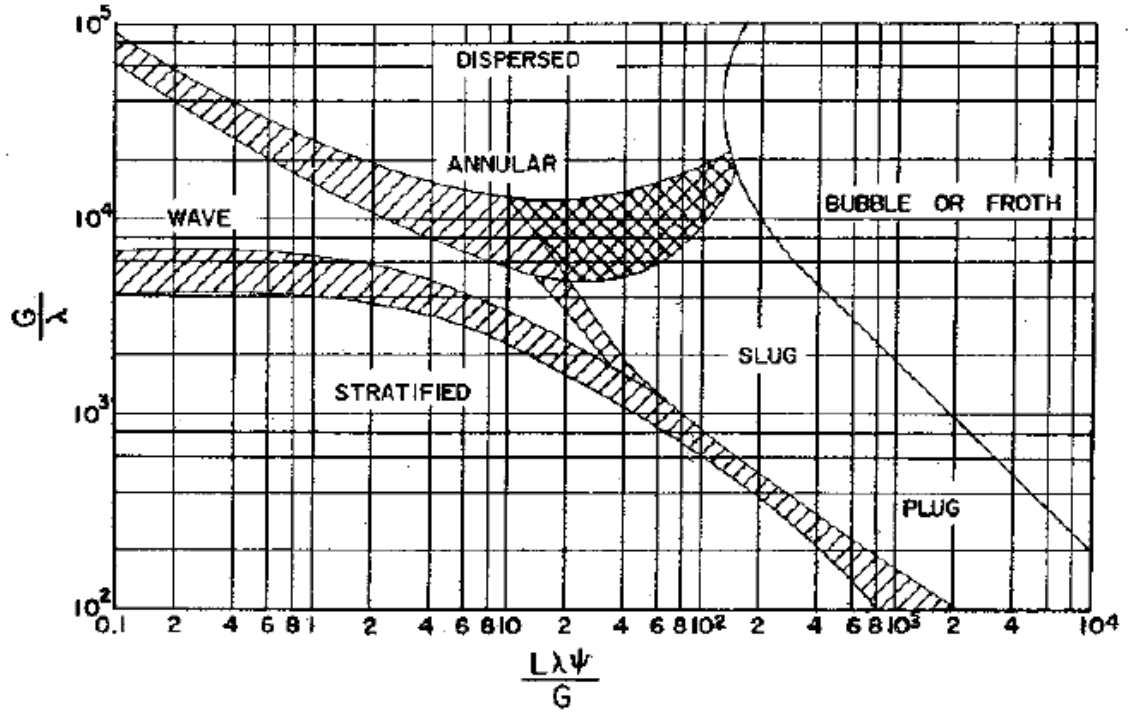


Figure 2.4 Modified Baker's Flow Pattern Map for Different Sizes Horizontal Pipelines Adapted from Reference[11]

Bell et al. (1970)[14] were modified the Baker's flow regime map and simplified the coordinates used by Baker. Figure 2.5 shows Baker's map modified by Bell et al. (1970), where X-axis: $G_L \Psi \left[\frac{cm \cdot lb^{\frac{2}{3}}}{dyne \cdot h^{\frac{4}{3}} \cdot ft^{\frac{1}{3}}} \right]$

and Y axis: $\frac{G_v}{\lambda} [ft/h]$

Where,

$$G_L = L = \frac{m_L}{S} \left[\frac{lb}{h \cdot ft^2} \right] \quad (5)$$

$$G_v = G = \frac{m_G}{S} \left[\frac{lb}{h \cdot ft^2} \right] \quad (6)$$

$$\Psi = \frac{1}{\sigma_L} [\mu_L \rho_L^2]^{1/3} [\text{cm ft}^{5/3} / \text{dyne h}^{1/3} \text{lb}^{1/3}] \quad (7)$$

$$\Lambda = [\rho_L \rho_G]^{1/2} [\text{lb/ft}^3] \quad (8)$$

Where the G_L and G_v are superficial mass velocities for liquid and gas phases respectively. The variables Λ and Ψ were introduced by Baker into coordinates to adjust the error in results coming from fluid properties. Better figure

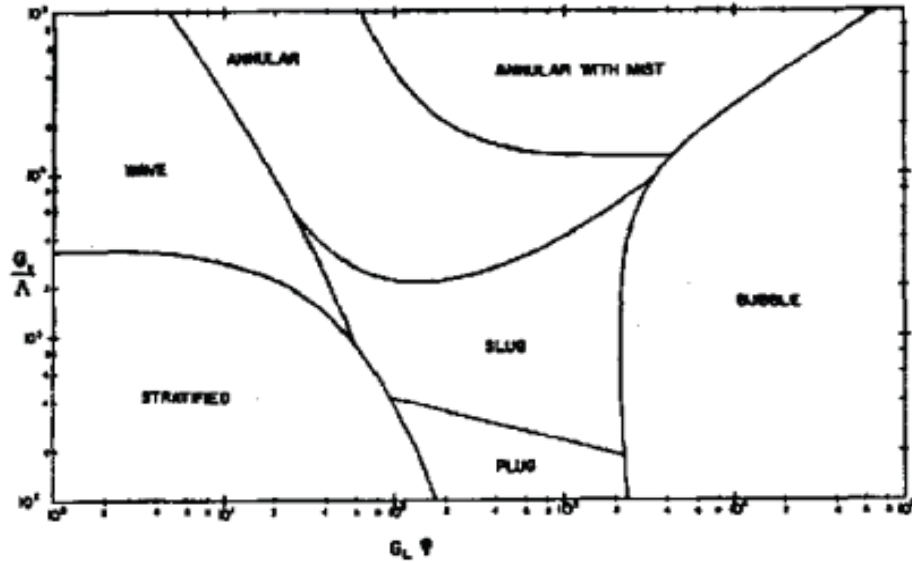


Figure 2.5 Modified Baker's Flow Regime Map for Horizontal Pipelines Adapted from Reference [14]

Whalley (1987)[15] repeated same Bell's work for horizontal pipelines but with SI units as shown in Figure 2.6. The axes in this figure are introduced as a combination of both of Bell's and Baker's coordinates.

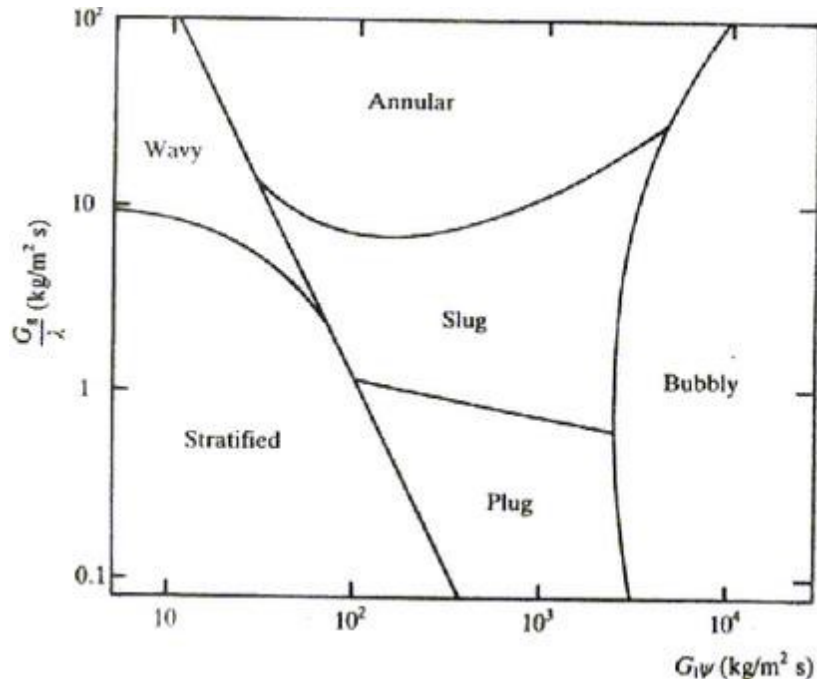


Figure 2.6 Modified Baker's Flow Regime Map for Horizontal Pipelines Adapted from Reference [15]

Hoogendoorn (1959)[12] studied two-phase flow for both systems air-oil and air-water in horizontal pipes with different diameters up to 5 cm. As a result of this study, a flow regime map was improved from which the flow regimes for these mixers can be predicted for the pipe diameter ranges explored in this work. Effect of some parameters such as pipe diameter, pipe roughness and fluid properties on transition lines in maps were explored in this study. The obtained results indicated that fluid properties and pipe diameter did not influence the flow regimes map.

Eaton et al. (1967)[16] developed a new flow regime map that used to predict the various flow regimes. They utilized experimental data gathered from gas-liquid system flows through two horizontal pipes, 2 and 4 inches, to develop this map. These experimental data were gained using distillate water or crude oil as aqueous phase and natural gas as a gaseous phase.

Mandhane et al. (1974)[17] collected 5935 observations for two-phase flow, gas-liquid, in horizontal pipes. They tested these data against the commonly used flow regime maps for horizontal pipes; then, about 1178 observations were used to modify a horizontal flow regime map as shown in Figure 2.7. Liquid and gas superficial velocities were used as mapping parameters in this study. The results indicated that fluid properties and pipe diameter have minimal impact on the boundaries transition of the flow patterns when the superficial velocities used as mapping parameters.

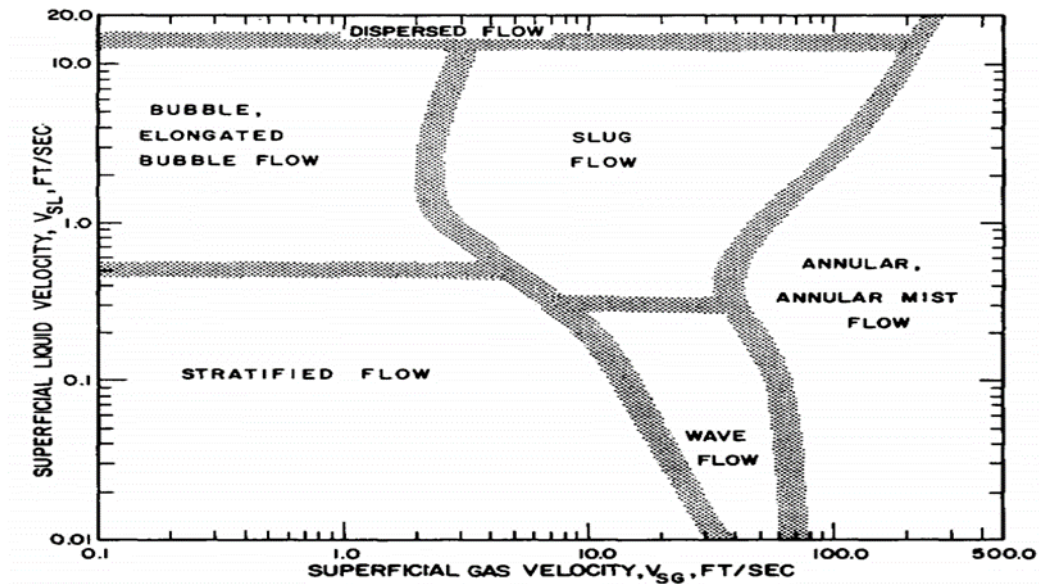


Figure 2.7 Mandhane Horizontal Flow Pattern Map [17]

In 1976, Taitel and Dukler[18] introduced a generalized flow pattern map based on the theory of the transition mechanisms. The proposed models capable to predict shift that can occur to transition lines during the variations in phase properties. They found that an important shift can be observed in the transition lines when phase properties are changed. Figure 2.8 shows this proposed flow regime map.

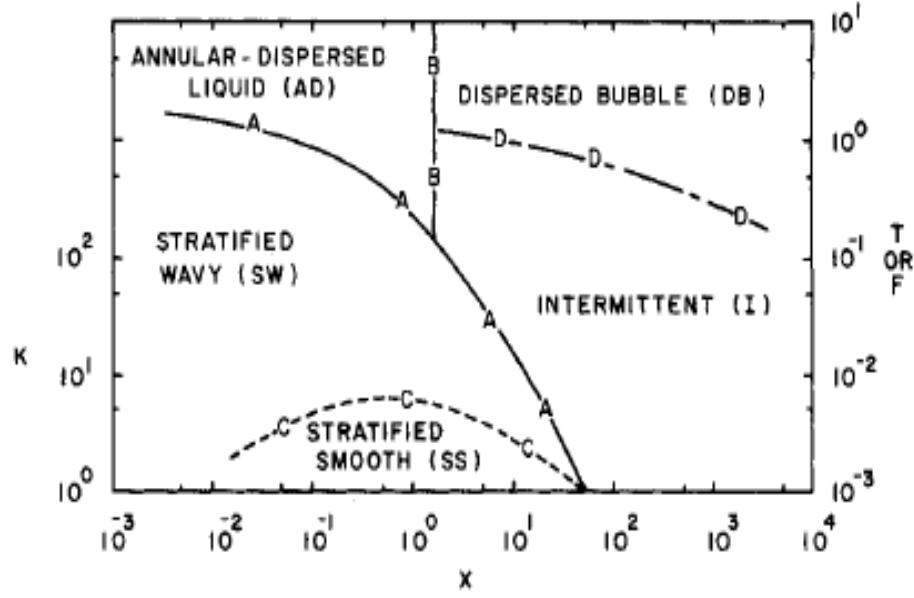


Figure 2.8 Taitel and Dukler's Flow Regime Map for Horizontal Pipe[18]

This map was drawn depending on the semi-theoretical concept, and it seems more complicated to use in comparison with other flow pattern maps. The parameters represented on axes can be calculated as the following:

$$X = \left[\frac{\frac{4C_L}{D} \left(\frac{\mu_L S^D}{V_L} \right)^{-n} \frac{\rho_L (\mu_L S)^2}{2}}{\frac{4C_G}{D} \left(\frac{\mu_G S^D}{V_G} \right)^{-m} \frac{\rho_G (\mu_G S)^2}{2}} \right]^{1/2} = \left[\frac{\left| \left(\frac{dP}{dX} \right)_L S \right|}{\left(\frac{dP}{dX} \right)_G S} \right]^{1/2} \quad (9)$$

$$F = \sqrt{\frac{\rho_G}{\rho_L - \rho_G} \frac{\mu_G S}{\sqrt{D g \cos \alpha}}} \quad (10)$$

$$K = F \left[\frac{D \mu_L S}{V_L} \right]^{1/2} = F [Re_L S]^{1/2} \quad (11)$$

The Lockhart-Martinelli parameter, X , depends on the all of C_L, C_G, n, m where the values of these parameters are taken at turbulent liquid flow ($n=m=0.2$, $C_L=C_G=0.046$).

Weisman et al. (1979)[19] explored the flow regime for the gas-liquid system in horizontal pipes. In this work, both of pipe diameter and fluid properties were investigated in horizontal pipes. New flow patterns transition data obtained from this study and other references data were compared with most commonly available transition correlations. The new data indicated that previous correlations[10], [17], [18], [20] were not accurate. Revised correlations were introduced based on new data of pipe diameter and fluid properties. Figure 2.9 shows the comparison between the results of Weisman et al.¹⁹ with another map of Mandhane et al (1974)[17]. From this figure, it can be clearly seen that surface tension has a significant impact on the boundary transition because the axes that were suggested by Taitel and Dukler[18] did not consider the influence of surface tension of the liquid. Also, Weisman et al.[19] concluded that the transition lines can be shifted slightly due to viscosity change, while the model of transition for intermittent regime introduced by Taitel and Dukler[18] suggests significant difference for transition lines due to viscosity change.

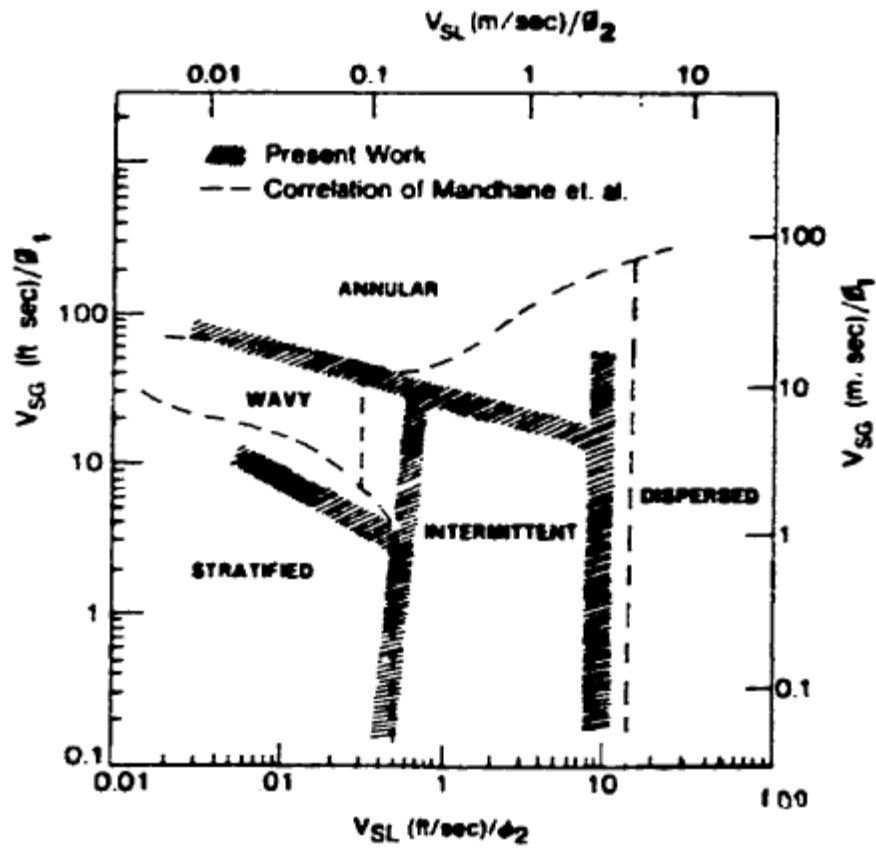


Figure 2.9 Horizontal Flow Pattern Map[19]

Spedding and Nguyen (1980)[3] developed flow regime maps using data of air-water two- phase flow system in 4.55 cm diameter for the entire pipe inclination range. They did not consider the effect of some parameters such as pipe diameter and fluid properties in this study, leading to less accuracy for these flow regime maps when they applied in other systems. The obtained results for Spedding and Nguyen[3] study is presented in Figure 2.10. The main categories for flow regime were separated with solid lines while each one of these categories was subdivided into smaller areas with broken lines.

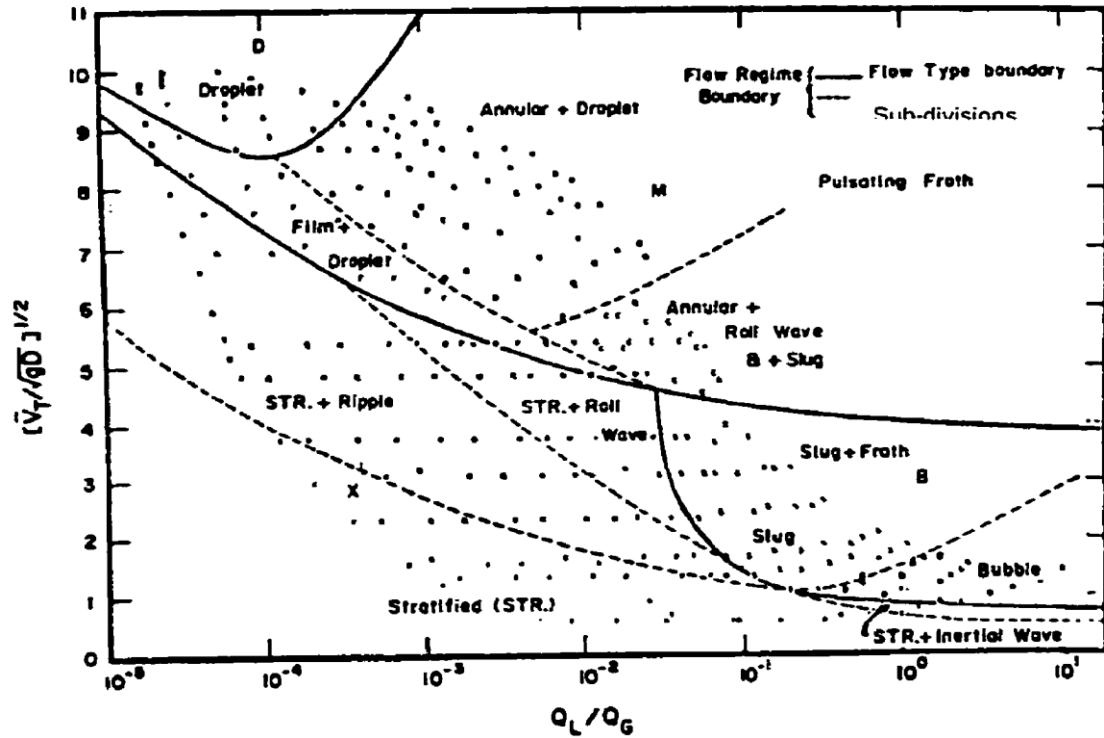


Figure 2.10 Flow Pattern Map[3]

Barnea et al. (1980)[21] presented a study for air-water two-phase flow. Two pipe diameters, 2.55 and 1.95 cm, were utilized in this work. The obtained results of this study were compared with the theoretical map generated from Taital and Dukler (1976)[18] study. Good agreement of experimental results with theory has been investigated from this study.

Barnea et al. (1983)[22] presented a study of the gas-liquid system in small diameter pipes (0.4 to 1.2 cm). New data for flow pattern transition lines was obtained from this work. The experimental results obtained from this work were compared with data gathered from the literature for horizontal and vertical flow models. Results of this comparison indicated that this model is also valid for large and moderate diameter pipes with some exception for the transition of stratified-non-stratified in horizontal pipes. The

surface tension impact on flow through small pipe diameters has found to be important only in the stratified-slug transition in horizontal pipes.

Lin and Hanratty (1987)[23] presented a flow pattern map for horizontal flow for the air-water system. The experimental data was measured at atmospheric pressure with two different horizontal pipes, 2.54 and 9.53 cm. The results obtained from this work indicated that pipe diameter does not affect the transition lines at high gas flow rates. In addition, the stratified to annular transition is different in small diameters than large diameters because of the influence of wave wetting. Figure 2.11 shows Lin and Hanratty' flow regime map.

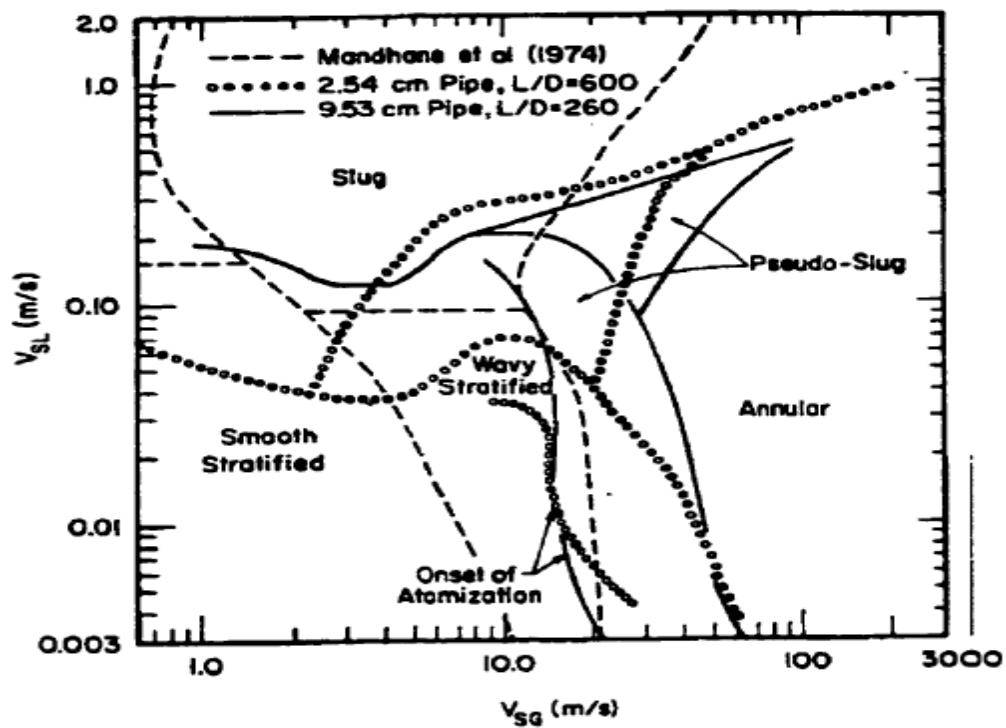


Figure 2.11 Comparison Between Two Flow Pattern Maps, one is introduced by Lin and Hanratty [23] and Other Suggested by Mandhane et al.[17]

Barnea (1987)[2] conducted a study of flow patterns in pipes. In this study, mechanism of transition and its applicability for a wide range of inclination angles of pipes have been explored. The explored mechanisms have been utilized to attain a dimensionless flow regime maps and an operative equation, where these equations and maps can be utilized to guess boundaries between the different flow patterns. All fluid properties, inclination angle and pipe size diameter were included in these equations or in a unified way to attain accurate model for flow patterns of two-phase flow. The flow regimes and the transition boundaries were shown in gas and liquid superficial velocities for air-water system flowing in a 1.97-inch diameter pipe. It was found that this model gave satisfactory results compared with real data for the range entire pipe inclinations range.

El-Oun (1990)[24] performed a combined work consists of theoretical and experimental data to study gas-liquid flow regimes in horizontal pipes. The experiments were conducted on 0.2 and 0.4 m diameter, 400 m long loops for a superficial velocity of air and water ranges up to 24 m/sec and 2 m/sec, respectively. The obtained results have shown excellent matching between experimental and prediction results of the transition lines and flow regime maps were improved based on visual observation for a vast range of air and water superficial velocities.

Spedding and Spence (1993)[25] conducted a study of two-phase gas-liquid flow regimes. The researchers conducted several experiments on air-water system flowing through horizontal pipes with 0.0935 m diameter to obtain experimental data. Different parameters such as visual observation, pressure drop and holdup data were combined together to identify the flow regimes. The experimental results of this work were utilized with previous work, at 0.0454 m pipe diameter, to examine the flow pattern maps.

Unfortunately, some of these maps were unable to obtain accurate results for flow regimes in both diameters.

Lee et al. (1993)[26] presented a study of boundary transition of the flow patterns for three-phase carbon dioxide- oil- water in 10 cm plexiglass horizontal pipe. It was found that the transition of flow patterns differs extremely from those for gas-liquid and oil-water flow systems. Flow pattern map for carbon dioxide-oil-water was developed from this study and it was compared with two-phase water-carbon dioxide and oil-water flow regime maps and compared with Taitel and Dukler model. From this study, it was found that liquid compositions have a significant impact on flow regime transitions.

Hand and Spedding (1993)[27] conducted a two-phase study for air-liquid flow in (0.0935 m inner diameter) horizontal pipe at atmospheric conditions. Glycerin was added to water to get a viscous solution, dynamic viscosities up to 0.1 Nsm^{-2} (100cp), to check the effect of viscosity on flow regime. The experimental data obtained from this work were used to compare theoretical and empirical flow pattern transition criteria. Flow regime maps that introduced by Lin and Hanratty and Anritos presented a good prediction of flow pattern for the air-water system and air-glycerin solution system respectively. It was found that the changes in liquid viscosity and pipe diameter were not handled by most theoretical transitions criteria. Wong and Yau (1997)[5] conducted a study for flow patterns transition in (10 m long, 25.4mm diameter) two-phase air-water horizontal flow system. In their study, sixteen different flow regimes were recognized depending on experimental observations using the high-resolution camera.

In 1999, Coleman and Garimella[28] presented the work to study the impacts of tube diameter and shape on two-phase flow. The gas and liquid superficial velocities range from 10 m/sec up to 100 m/sec, respectively. Flow pattern maps were developed for a small round and rectangular diameter. It was found that diameter and surface tension had considerable effects on flow patterns and boundaries transition for less than 10 mm diameter.

In 2003, Spedding et al.[29] performed a study on two-phase flow in horizontal pipes. From this study, a new flow regime map was developed for liquid viscosity less than 0.02 kg/m.s. They were tested their map against a large set of data and they found that the map showed good agreement with these data under various operating conditions and phase properties. In addition, boundary transition of this map has good agreement with other flow models.

Benard and Spedding (2006)[30] developed a universal flow pattern map. Dimensionless mapping parameters used in this map allowed for accurate estimation of the presence of the stratified roll wave pattern in the two-phase horizontal flow. Boundary transition to the rolling wave from other flow patterns was presented in this study.

Gokcal et al. (2008)[31] presented a study to explore the effect of viscous crude oil on flow regimes for oil-gas flow regime in horizontal pipes. Experiments were conducted on a 5.08 cm inner diameter and 1890 cm long horizontal pipe. Gas and liquid superficial velocities range from 1.75 m/sec up to 20 m/sec, respectively. Oil viscosity ranges from 181 cp to 587 cp. The results of this study were used to evaluate the validity of existing

flow patterns models. It was concluded that at high oil viscosity significant discrepancies were observed on existing flow regimes.

Oliveira et al. (2010)[32] presented a study of flow patterns visualization for two-phase in horizontal and inclined tubes. 1-inch diameter transparent acrylic tube was used in this study. Water used as a liquid phase with superficial velocity ranges up to 3.28 m/sec and air used as a gas phase with superficial velocity ranges up to 5.48 m/sec. It was concluded that Mandhane et al.[17] experimental map and the Taitel and Dukler[18] theoretical map have a perfect agreement with the real data attained from this study.

Tzotzi et al. (2010)[33] presented a study to investigate the effect the gas density and surface tension on flow regimes transition in horizontal pipes. Experiments were performed in a 1275 cm long pipe with a 2.4 cm diameter at atmospheric conditions. CO₂ and He gases were used to conduct gas density effect while aqueous solutions were used to conduct the surface tension effect. It was concluded that surface tension and gas density highly affected on the boundaries transition.

Ba geri et al. (2017)[34] studied the effect of surface tension on flow regimes for two-phase in horizontal pipes. The experiments were conducted on 1-inch diameter horizontal steel pipe, where liquid superficial velocity ranged 0.2 to 1.6 ft/min and gas superficial velocity ranged 0.7-3.3 ft/sec. It was concluded that the effect of surface tension is more distinct on the low gas-liquid velocities and the boundary between the elongated bubble and the plug flow pattern is shifted due to a reduction in the surface tension. The effect of surface tension was diminished at high gas and liquid velocities.

CHAPTER 3

METHODOLOGY

3.1 Experiment Description

3.1.1 Flow Loop Set-up

The flow loop set-up that was used to conduct the flow regime experiments consist of a centrifugal pump with variable speed drive (VSD), steel tank, gas compressor with an air=dryer, 1-inch diameter horizontal PVC pipe 6 m length with a 1-meter length of plexy-glass pipe, two liquid flow meters, two gas flow meters, two pressure gauges, differential pressure gauge and high-resolution camera. Figure 3.1 and Figure 3.2 show the flow loop with a schematic diagram.

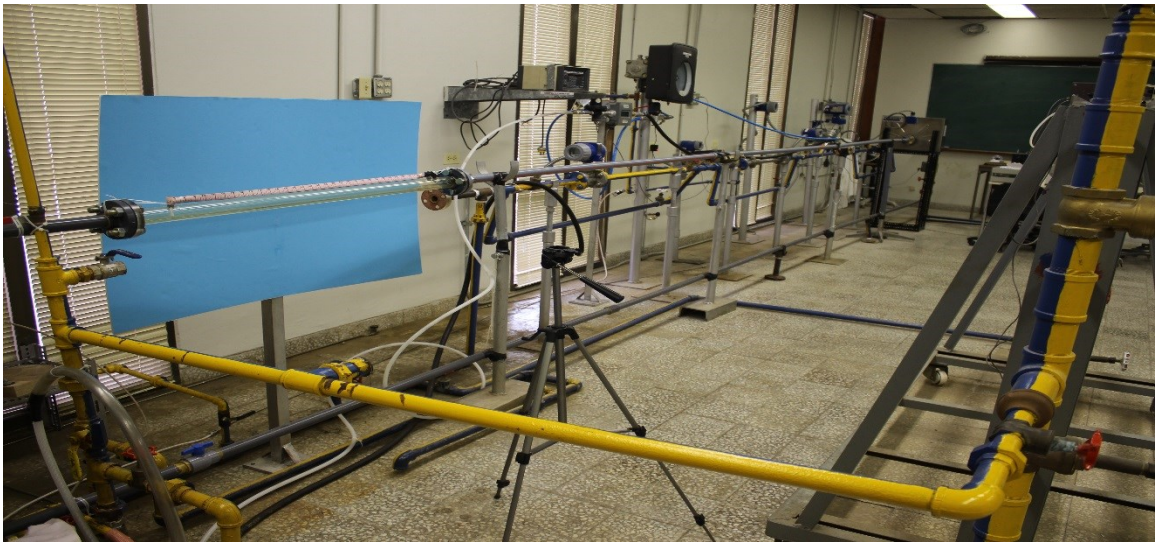


Figure 3.1 Horizontal Flow Loop

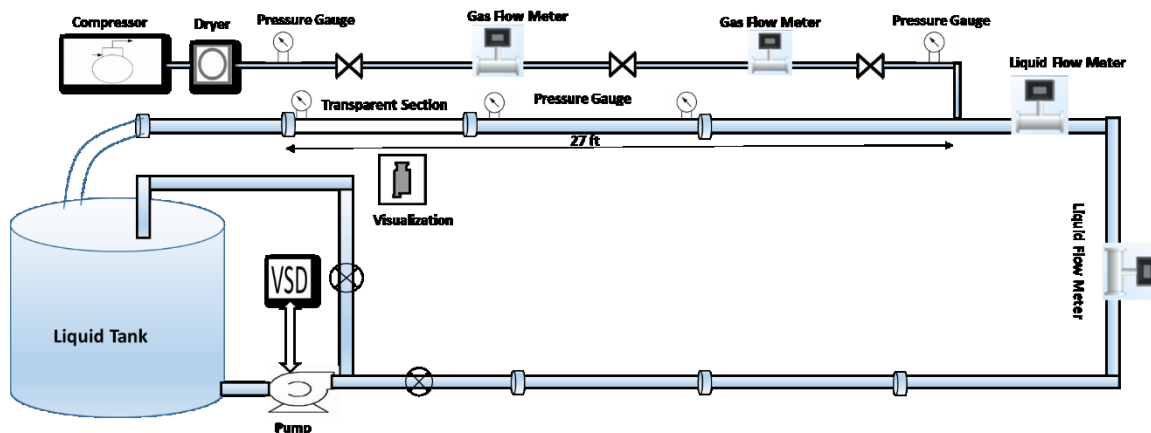


Figure 3.2 A Schematic of the Horizontal Flow Loop

A centrifugal pump was used to pump the liquid to the flow loop and two liquid flow meters were used to measure the liquid flow, one flow meter for low liquid flow rate 1.5-15 liter/min and the second flow meter were used for high liquid flow rate 15-96.5 liter/min. While, air compressor was used to provide the air to the flow loop and two gas flow meters were used to measure the gas flow rate, one flow meter used for low gas flow rate 0.35-7 scf/min and the second flow meter used for high gas flow rate 7-20 scf/min. The liquid flow rates were controlled using variable speed drive and by-pass valve and gas flow rates were controlled by using the pressure regulators using needle valve installed at upstream and downstream of the pressure regulator. Two pressure gauges were used to measure the pressure at inlet and outlet for 7 ft of the pipe length and differential pressure gauge used to measure the pressure drop for same 7 ft pipe length.

3.1.2 Preliminary Measurements

3.1.2.1 Surface Tension Measurements

Four different concentrations of surfactant (Alpha Olefin Sulfonate (AOS)) were used to evaluate the effect of surface tension on two-phase flow regimes in horizontal pipes. A Du Nouy ring tensiometer was used to measure surface tension at room conditions. Table

3.1 shows the four surfactant concentrations that used in the flow regime experiments. Surfactant concentration (%) was plotted versus surface tension to determine surfactant concentration required to obtain the desired value of surface tension as illustrated in Figure 3.3. The critical micelle concentration was determined to avoid an extra addition of the surfactant with no further change in the surface tension.

Table 3.1 Surface Tension, Viscosity and Density Measurements of Different Surfactant Concentrations

Surfactant Concentration (Vol %)	Surface Tension(mN/m)	Viscosity (cP)	Density (gm/cc)
0	70.5	1	1
0.02	59.7	1	1
0.05	55.8	1	1
0.1	46.5	1	1
0.5	32.4	1	1
0.6	32.4	1	1

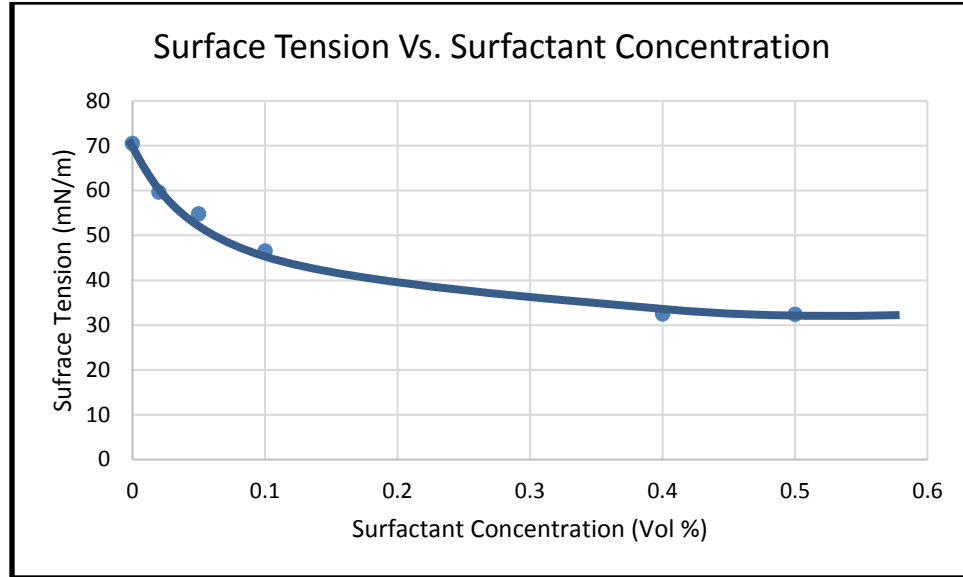


Figure 3.3 Surfactant Concentrations (Vol %) versus Surface Tension (mN/m)

3.1.2.2 Viscosity Measurements

Four different concentrations of glycerin were used to evaluate the effect of viscosity on two-phase flow regimes in horizontal pipes. Ostwald viscometer was used to measure the viscosity of the solution at room conditions. Table 3.2 shows the four glycerin concentrations that were used for evaluating the viscosity effect on two-phase flow regimes in horizontal pipes.

Table 3.2 Viscosity, Surface tension and Density Measurements of Different Surfactant Concentrations

Glycerin Concentration (Vol %)	Viscosity (cP)	Surface Tension(mN/m)	Density (gm/cc)
0	1	70.5	1
5	1.27	66.5	1
10	1.41	64	1
20	1.87	57.3	1
30	3.10	55.4	1

3.1.2.3 Density Measurements

Two different concentrations of (Calcium Bromide and Surfactant) were used to evaluate the effect of density on two-phase flow regimes in horizontal pipes. Pycnometer was used to measure the density of the solution at ambient conditions. Table 3.3 shows the two concentrations that used for evaluating the density effect on two-phase flow regimes in horizontal pipes.

Table 3.3 Density, Surface tension and Viscosity Measurements of Different (CaBr₂ with Surfactant) Concentrations

CaBr₂-Surfactant (Vol%)	Density (gm/cc)	Surface Tension(mN/m)	Viscosity (cP)
0	1	70.5	1
25% +0.004%Surf	1.2	61.6	1.44
75%+0.02%Surf	1.5	56.3	2.95

3.1.3 Experiment Procedure

The strategy applied to the flowing experiments was by fixing the liquid flow rate and changing gas flow rates from low to high in a stepwise manner. Then the gas flow rate was reduced in a stepwise manner to analyze the hysteresis effect. The procedure was followed for the range of liquid flow rate. Table 3.4 summarizes the flow rates (Q_p) and superficial velocities (V_{sp}) of phases used in the flowing system. The flow patterns were captured through the transparent section of the pipe using the high-resolution camera at steady-state for individual changes in gas and liquid rate. These experiments were repeated for the range of the fluid properties considered in this study. The effect of surface tension was evaluated by reducing the surface tension with the aid of surfactant while the effect of fluid viscosity has been evaluated by increasing fluid viscosity with aid of glycerin and the effect of density has been evaluated by increasing density with aid Calcium Bromide (CaBr_2) and small concentration of surfactant was added to reduce the surface tension of the solution to attain appropriate surface tension values for comparison. Four different cases (0.02, 0.05, 0.1, 0.5 vol %) of a surfactant were utilized to estimate the influence of the surface tension on the boundaries of different flow patterns. Four different concentrations (5, 10, 20, 30 vol %) of a glycerin were used to evaluate the effect of the fluid viscosity on the boundaries of different flow patterns. Two different concentrations of Calcium Bromide (CaBr_2) and surfactant were used to evaluate the effect of the fluid density on the boundaries of different flow regimes.

Table 3.4 Flowing Parameters

Parameter	Minimum value	Maximum value
Q_L(Liter/min)	1.5	96.5
V_{sl}(ft/sec)	0.16	10.42
Q_L(Scf/hr)	21.18	1200
V_{sg}(ft/sec)	1.07	61.14

3.2 Data Analysis

A large set of experimental data was collected by capturing the flow patterns through the transparent section using the high-resolution camera at all the range of gas and liquid superficial velocities that were used in the experiments. The experimental data was utilized to generate flow pattern map and the effect of surface tension, fluid viscosity, and fluid density were evaluated based on the variation in the boundaries of different flow patterns.

CHAPTER 4

RESULTS AND DISCUSSION

Flow regime maps were developed using the experimental data and the visualization through the transparent section of the pipe. The effects of surface tension, fluid viscosity, and fluid density were evaluated based on the variation in the boundaries of different flow patterns. Furthermore, Pressure drop maps were developed using the pressure drop data that collected from experiments of air-water system, air-0.5 vol % surfactant system, air-30 vol % glycerin system, air-(25 vol % CaBr_2 -0.004 vol % surfactant) system and air-(75 vol % CaBr_2 -0.02 vol % surfactant) system.

4.1 Flow Regime Results

4.1.1 Base Case (Air-Water) System

For the base case, air and water were used as the gas and liquid phase for the flow experiment. The water flow rate was fixed at one value (example 1.5 liter/min) and air flow rate were changed from 20-1200 scf/hr then from 1200-20scf/hr. The surface tension of the air-water was 70.5 mN/m while viscosity and density are 1 cP and 1 gm/cc respectively. The flow pattern map has been developed by plotting gas superficial velocity on X-axis and liquid superficial velocity on Y-axis. Figure 4.1 shows the different flow regimes of air/water system while Figure 4.2 shows the effect of increasing gas superficial velocity at constant liquid superficial velocity ($V_{SL} = 2.67$ ft/sec). It is clearly seen that smooth stratified and wavy stratified were observed at low liquid superficial velocity while elongated bubble appears with an increase in liquid superficial

velocity at low gas superficial velocity. The increase in superficial velocity of gas plug, plug-slug, pseudo-slug, and slug were observed. Bubble flow and dispersed bubble were observed at a high liquid superficial velocity and low gas flow rate and annular flow were observed with increasing gas superficial velocity.

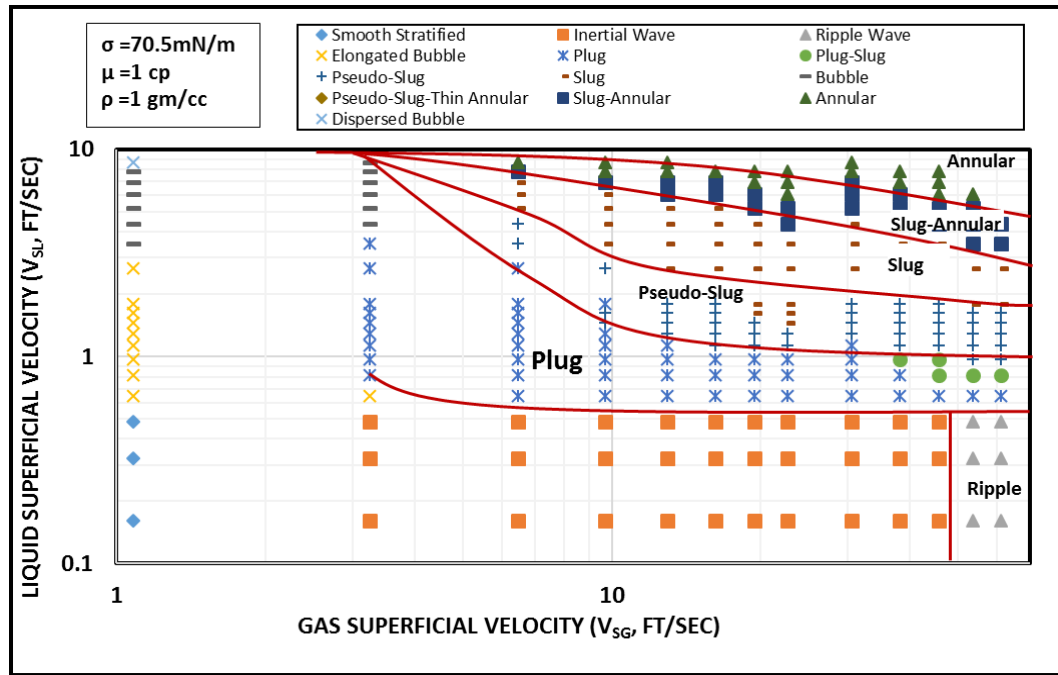


Figure 4.1 Flow Pattern Map of the Base Case (Air-Water)

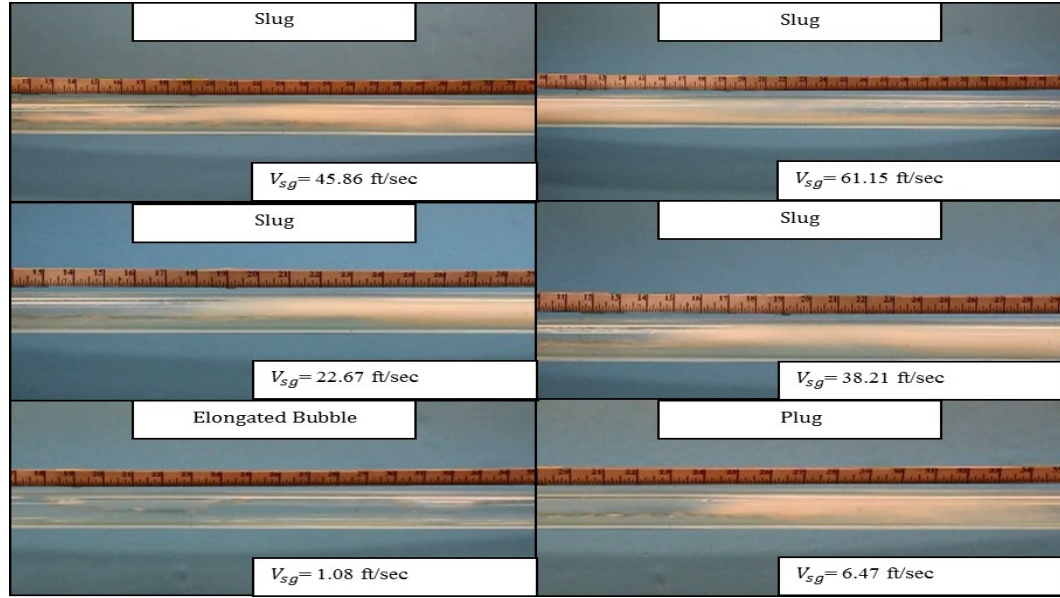


Figure 4.2 Effect of Gas Superficial Velocity of the Base case (Air-Water, $V_{SL} = 2.67$ ft/sec)

4.1.2 Effect of Surface Tension (σ)

4.1.2.1 Case I: 0.02 Vol % Surfactant Concentration ($\sigma = 59.7$ mN/m)

In this case, 0.02 vol % surfactant concentration was added to the water. The surface tension of the solution was 59.7 mN/m while viscosity and density was 1 cP and 1 gm/cc respectively. By comparing this case with base case, it can be seen that the boundary between ripple wave and inertial wave shifted to the left due to a reduction in the surface tension and more plug-slug flow was observed in this case compared with the base case. Figure 4.3 shows the different flow patterns of air/0.02 vol % surfactant concentration (surface tension 59.7 mN/m) and the effect of increasing gas superficial velocity at fixed liquid superficial velocity ($V_{SL} = 2.67$ ft/sec) is shown in Figure 4.4.

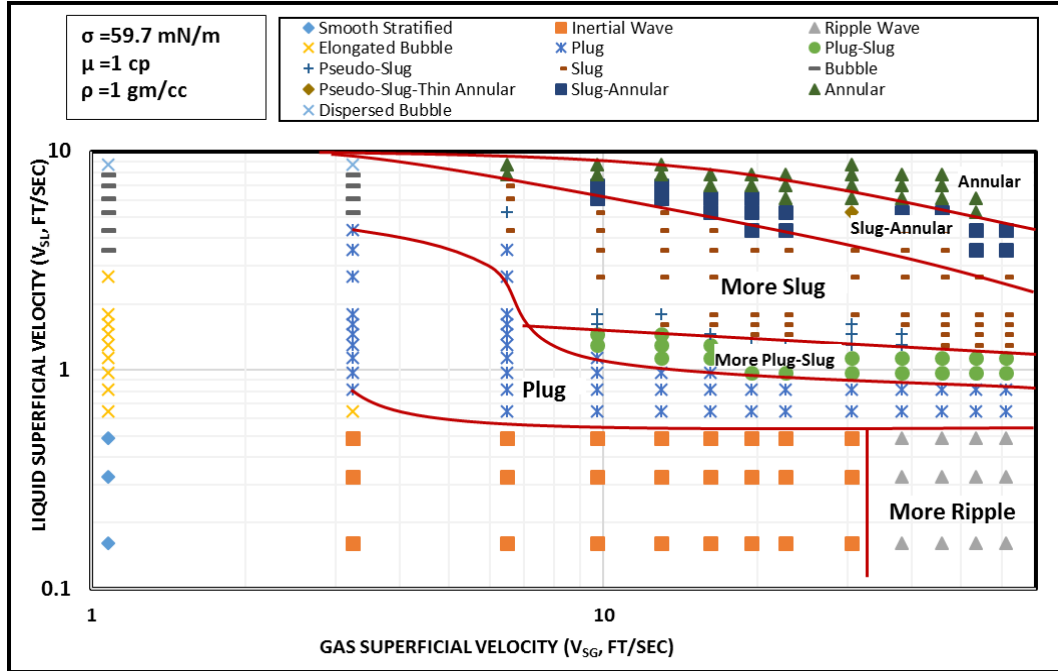


Figure 4.3 Flow Pattern Map of the (Air-0.02 Vol % Surfactant Concentration)

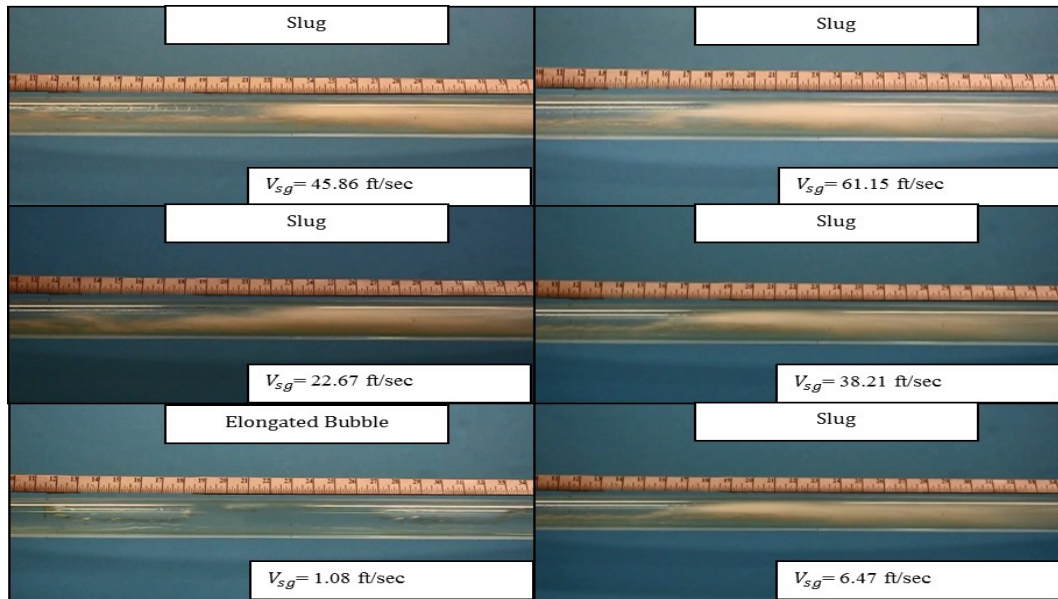


Figure 4.4 Effect of Gas Superficial Velocity of the (Air-0.02 Vol % Surfactant Concentration, $V_{SL}= 2.67$ ft/sec)

4.1.2.2 Case II: 0.05 Vol % Surfactant Concentration ($\sigma = 54.8$ mN/m)

In this case, 0.05 vol % surfactant concentration was added to the water. The surface tension of the solution was 54.8 mN/m while viscosity was 1 cP and density 1 gm/cc. By

comparing this case with base case, it can be seen that boundary between ripple wave and inertial wave shifted to the left due to a reduction in the surface tension and more slug flow was observed in this case compared with the base case and the case of 0.02 vol % surfactant concentration. Figure 4.5 shows the different flow patterns of air/0.05vol % surfactant concentration (surface tension 54.8 mN/m) and the effect of increasing gas superficial velocity at fixed liquid superficial velocity ($V_{SL} = 2.67$ ft/sec) is shown in Figure 4.6.

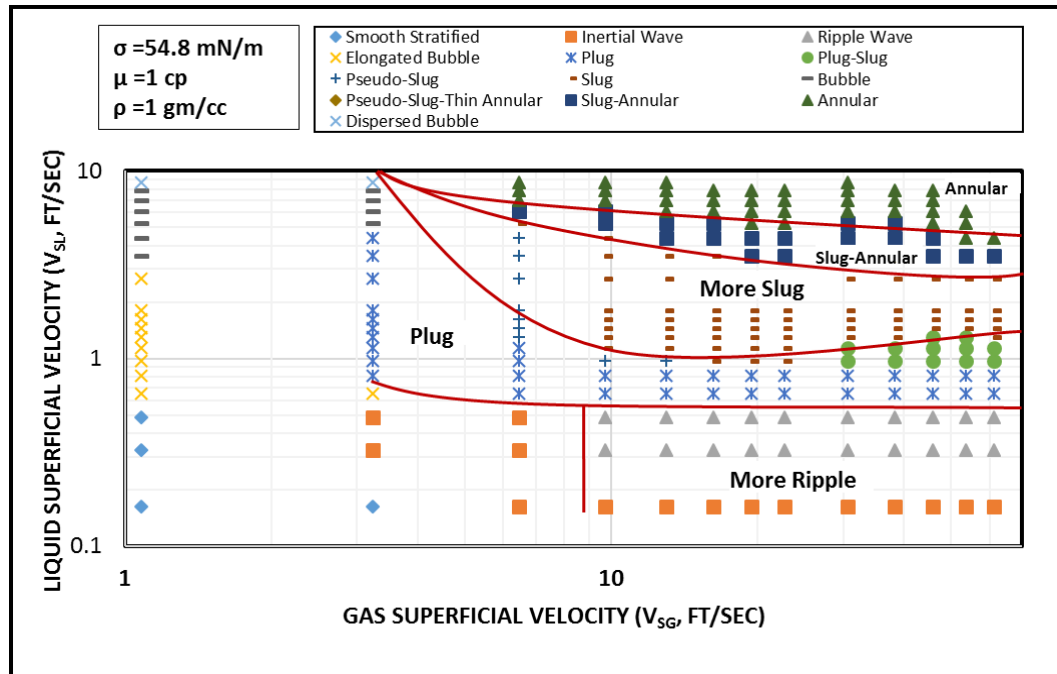


Figure 4.5 Flow Pattern Map of the (Air-0.05 Vol % Surfactant Concentration)

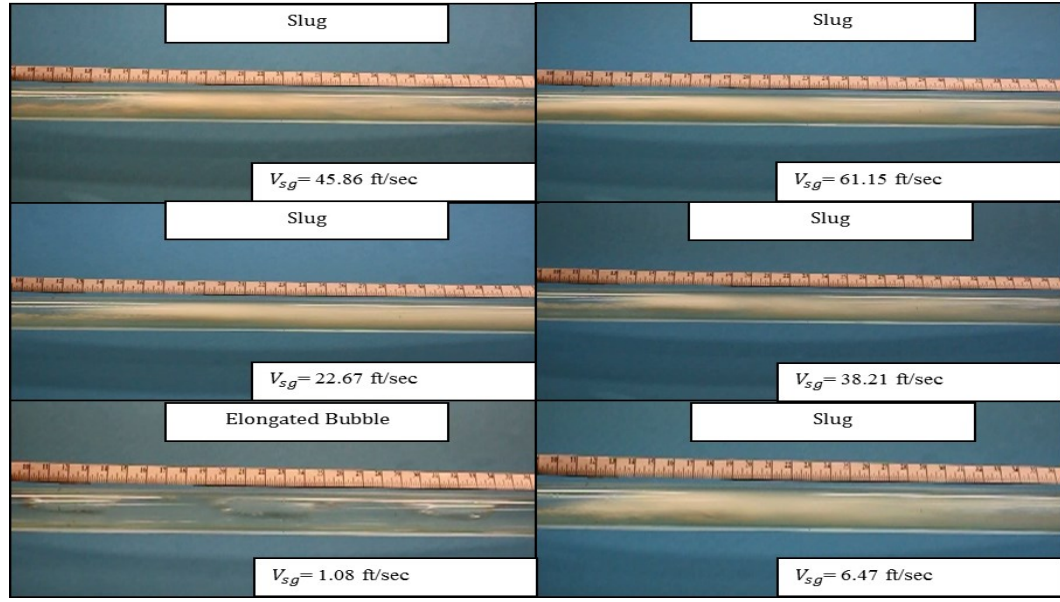


Figure 4.6 Effect of Gas Superficial Velocity of the (Air-0.05 Vol % Surfactant Concentration, $V_{SL} = 2.67$ ft/sec)

4.1.2.3 Case III: 0.1 Vol % Surfactant Concentration ($\sigma = 46.5$ mN/m)

The 0.1 vol % of surfactant solution was used in this case as the liquid phase. At this surfactant concentration, the surface tension was 46.5 mN/m while viscosity and density still constant at 1 cP and 1 gm/ cc, respectively. The distinct effect is that more slug-annular flow was observed at high liquid and gas superficial velocities compared with the base case and the higher surface tension cases (lower surfactant concentration). Figure 4.7 shows the different flow patterns of air/0.1 vol % surfactant concentration (surface tension 46.5 mN/m) and the effect of increasing gas superficial velocity at fixed liquid superficial velocity ($V_{SL} = 2.67$ ft/sec) is shown in Figure 4.8.

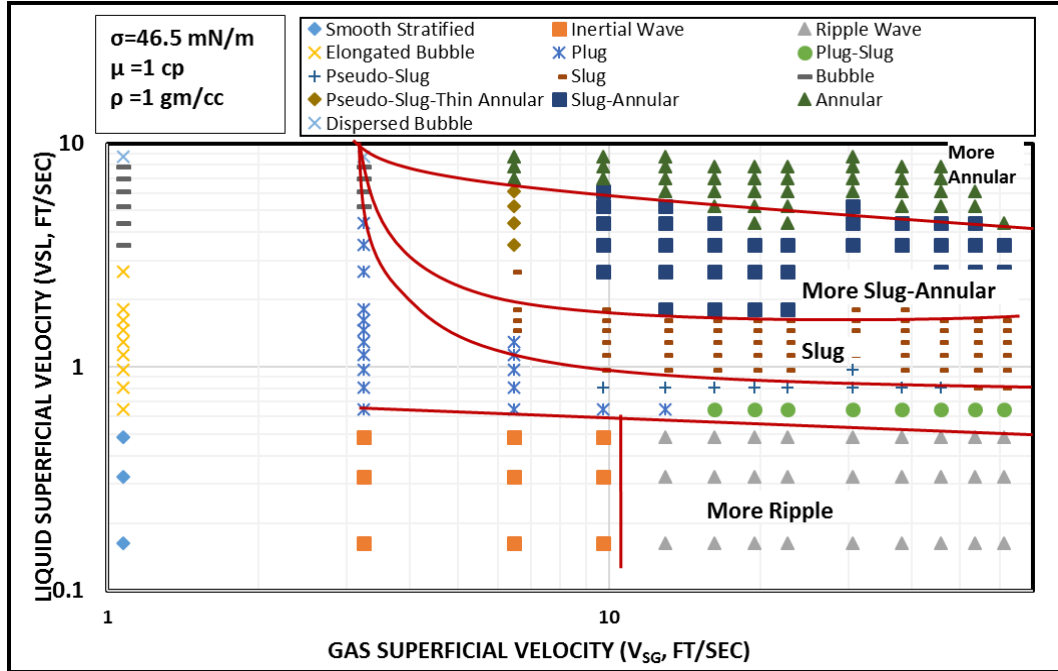


Figure 4.7 Flow Pattern Map of the (Air-0.1 Vol % Surfactant Concentration)

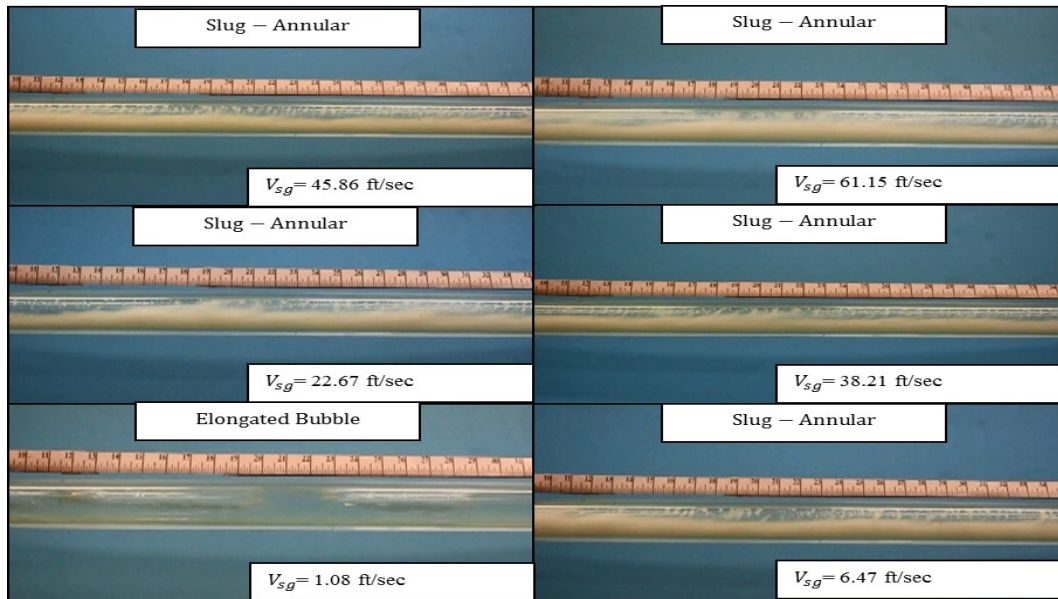


Figure 4.8 Effect of the gas superficial velocity of the (Air-0.1 Vol % Surfactant Concentration, $V_{SL} = 2.67$ ft/sec)

4.1.2.4 Case IV: 0.5 Vol % Surfactant Concentration ($\sigma = 32.4$ mN/m)

The 0.5 vol % of surfactant solution was used in this case as the liquid phase. At this surfactant concentration, the surface tension was 32.4mN/m (CMC) while viscosity and

density are still constant i.e. 1 cP and 1 gm/cc, respectively. As can be seen in Figure 4.9, more slug-annular and annular flow were observed at high liquid and gas superficial velocities compared with base case and the higher surface tension cases. The effect of increasing gas superficial velocity at fixed liquid superficial velocity ($V_{SL} = 2.67$ ft/sec) is shown in Figure 4.10.

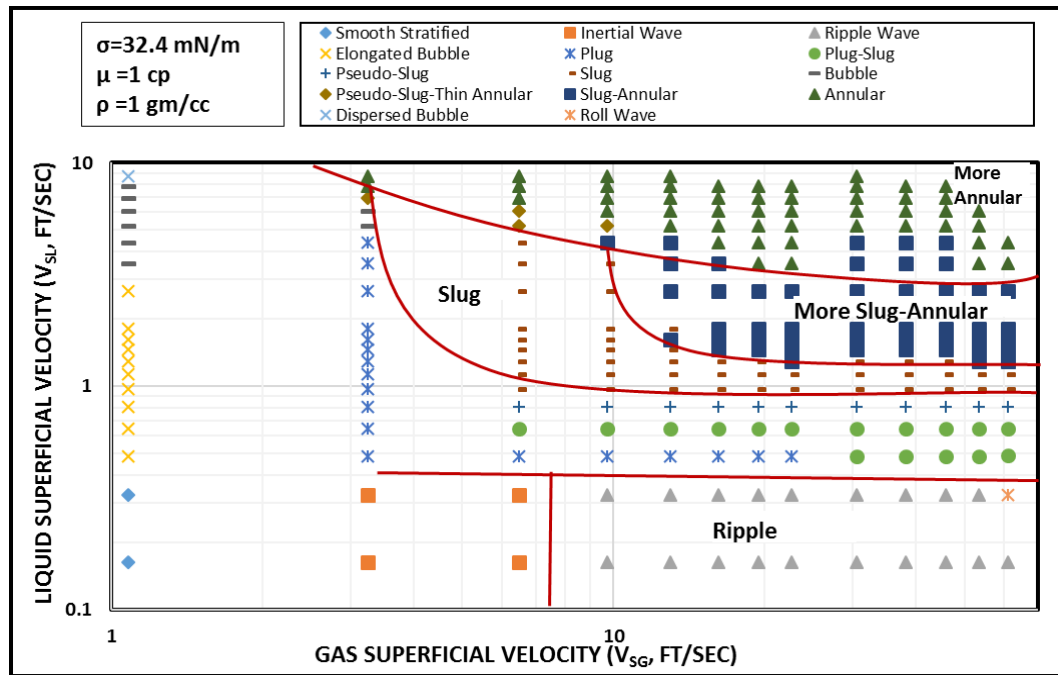


Figure 4.9 Flow Pattern Map of the (Air-0.5 Vol % Surfactant Concentration)

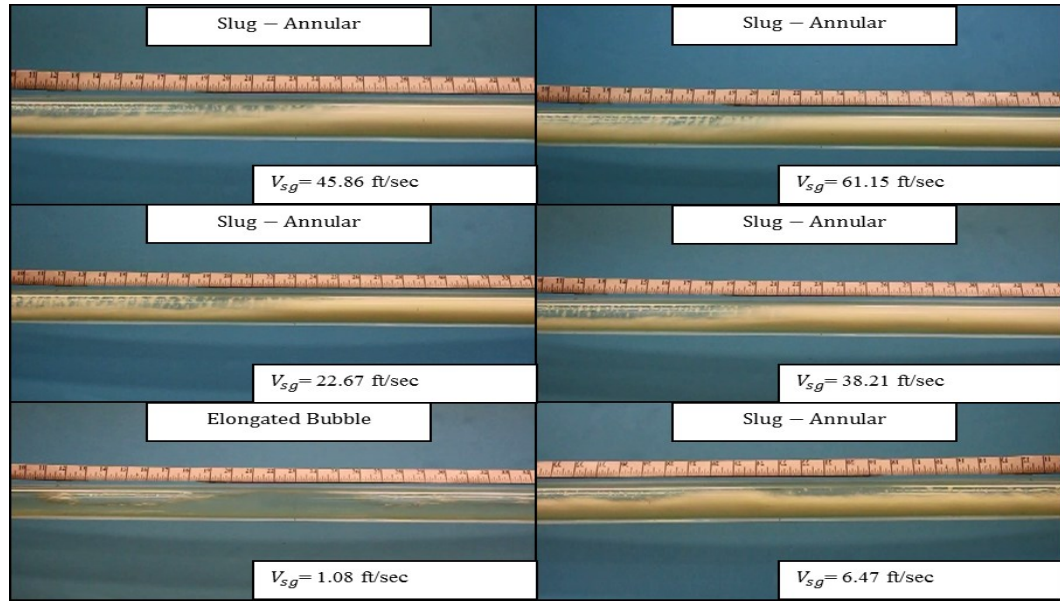


Figure 4.10 Effect of Gas Superficial Velocity of the (Air-0.5 Vol % Surfactant Concentration, $V_{SL} = 2.67$ ft/sec)

4.1.3 Effect of Viscosity (μ)

4.1.3.1 Case I: 5 Vol % Glycerin Concentration ($\mu = 1.27$ cP)

In this case, 5 vol % glycerin was added to the water. The viscosity of the solution was 1.27 cP while surface tension was 66.5 mN/m and density 1 gm/cc. By comparing this case with the base case, it is clearly seen that boundary between slug and pseudo-slug shifted down due to increasing the viscosity of the solution. Figure 4.11 shows the different flow patterns of air/5 vol % glycerin concentration and the effect of increasing gas superficial velocity at fixed liquid superficial velocity ($V_{SL} = 2.67$ ft/sec) is shown in Figure 4.12.

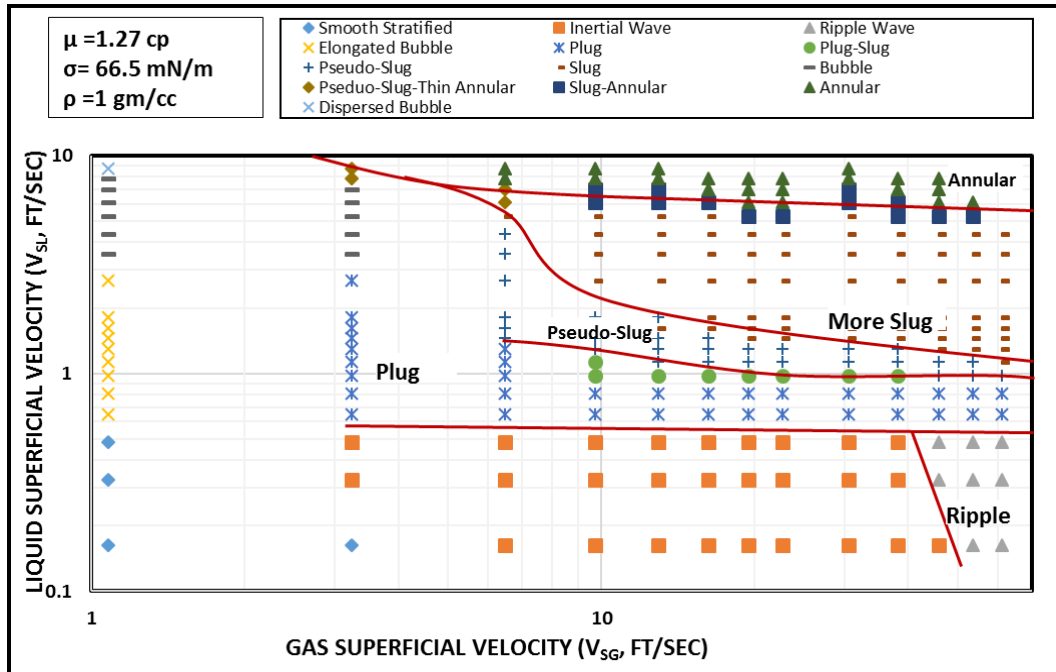


Figure 4.11 Flow Pattern Map of the (Air- 5 Vol % Glycerin Concentration)

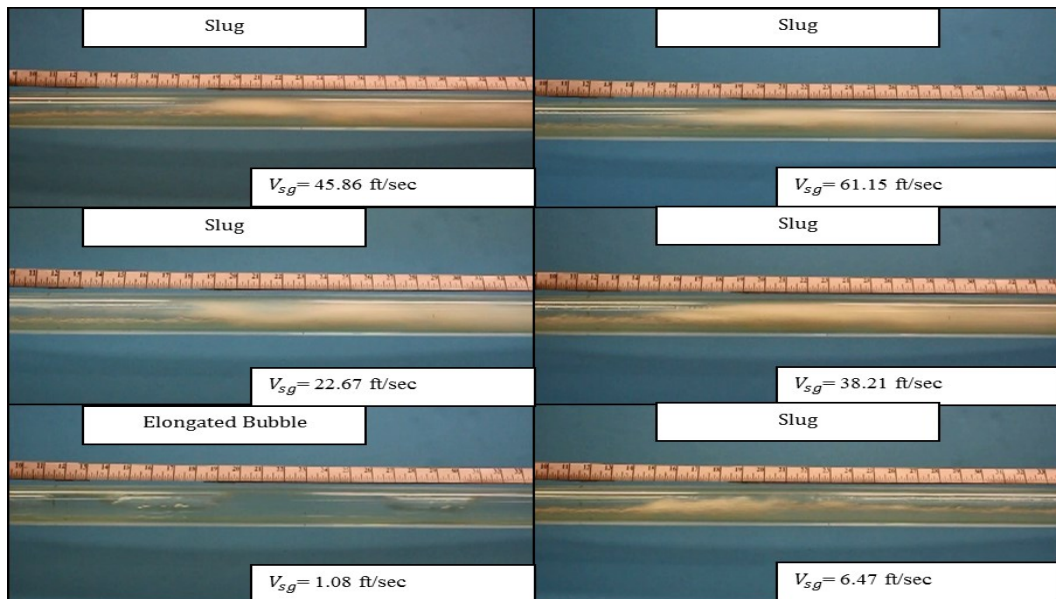


Figure 4.12 Effect of Gas Superficial Velocity of the (Air- 5 Vol % Glycerin Concentration, $V_{SL} = 2.67$ ft/sec)

4.1.3.2 Case II: 10 Vol % Glycerin Concentration ($\mu = 1.41$ cP)

In this case, 10 vol % glycerin concentration was added to the water. The viscosity of the solution was 1.41cP while surface tension was 63.98 mN/m and density 1 gm/cc. By

comparing this case with base case and 5% glycerin concentration case, it is clearly seen that boundary between ripple wave and inertial wave shifted to the left and the boundary between slug and pseudo-slug more shifted down due to increasing the viscosity of the solution. Also, the annular and slug-annular flow patterns appear in the flow regime map compared with the base case and 5 vol % glycerin concentration case for the gas and liquid velocity considered in this study. Figure 4.13 shows the different flow patterns of air/10% glycerin concentration and the effect of increasing gas superficial velocity at fixed liquid superficial velocity ($V_{SL}=2.67$ ft/sec) is shown in Figure 4.14.

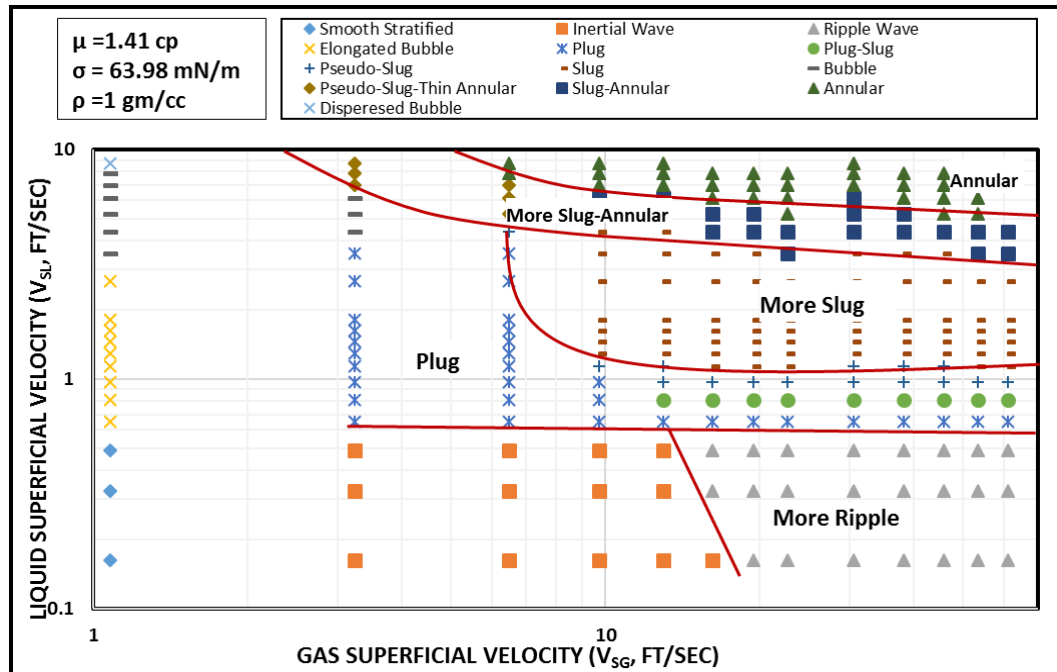


Figure 4.13 Flow Pattern Map of the (Air- 10 Vol % Glycerin Concentration)

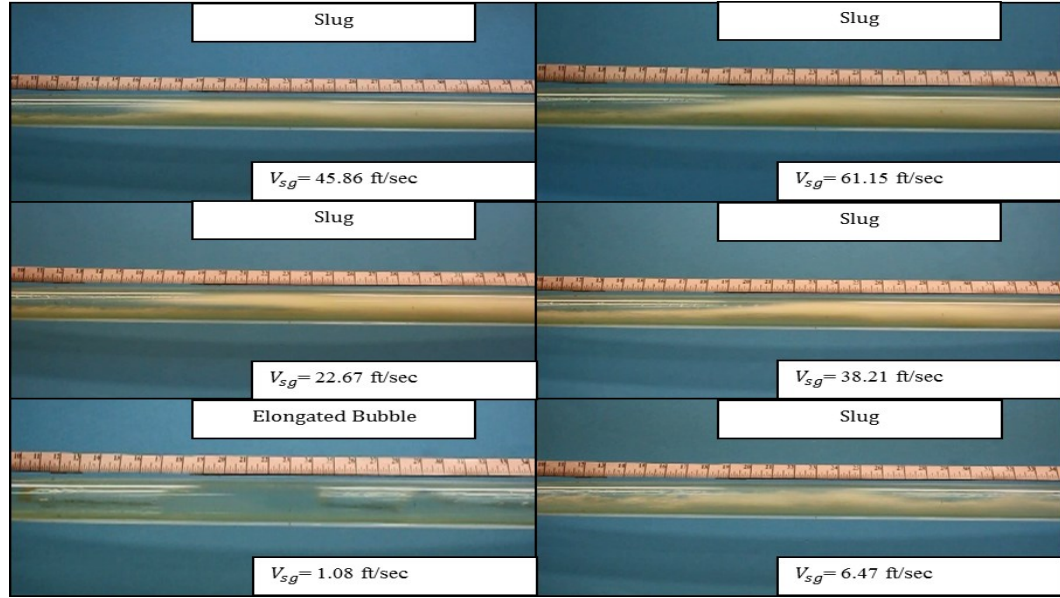


Figure 4.14 Effect of Gas Superficial Velocity of the (Air- 10 Vol % Glycerin Concentration, $V_{SL} = 2.67$ ft/sec)

4.1.3.3 Case III: 20 Vol % Glycerin Concentration ($\mu = 1.87$ cP)

The 20 vol % of glycerin was used in this case as the liquid phase. At this glycerin concentration, the viscosity of the solution was 1.87 cP, while surface tension was 57.3 mN/m and density still constant at 1 gm/ cc. As can be seen in Figure 4.15, more slug-annular and annular flow were observed at high liquid and gas superficial velocities compared with 0.02 vol % surfactant case that has almost same surface tension value and the boundaries between annular/slug-annular and slug-annular/slug flow shifted down due increasing in the viscosity. The effect of increasing gas superficial velocity at fixed liquid superficial velocity ($V_{SL} = 2.67$ ft/sec) is shown in Figure 4.16.

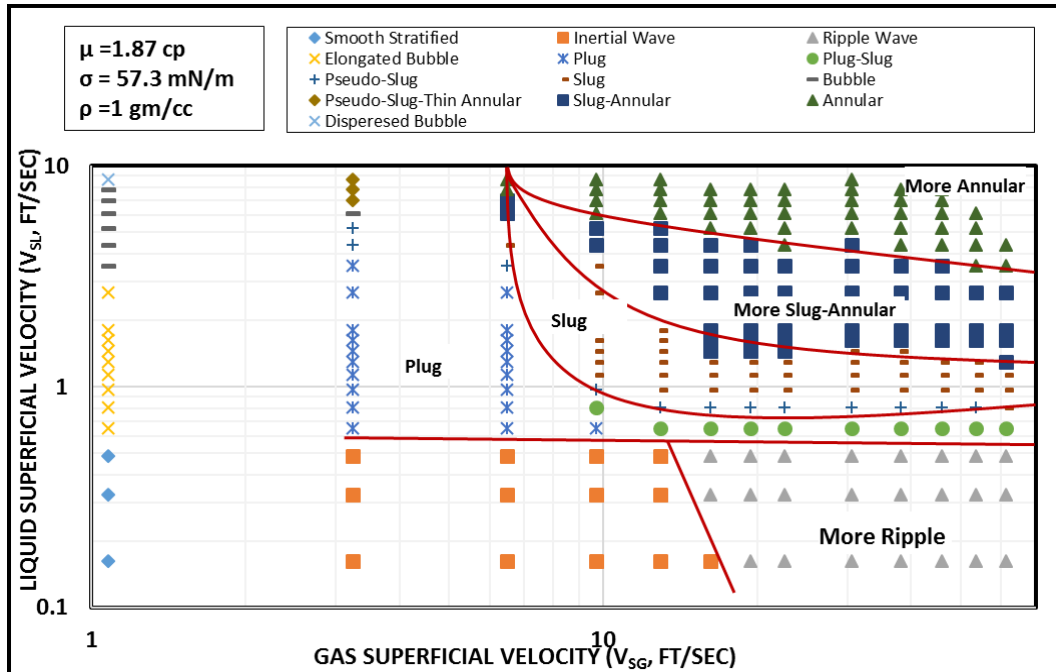


Figure 4.15 Flow Pattern Map of the (Air- 20 Vol % Glycerin Concentration)

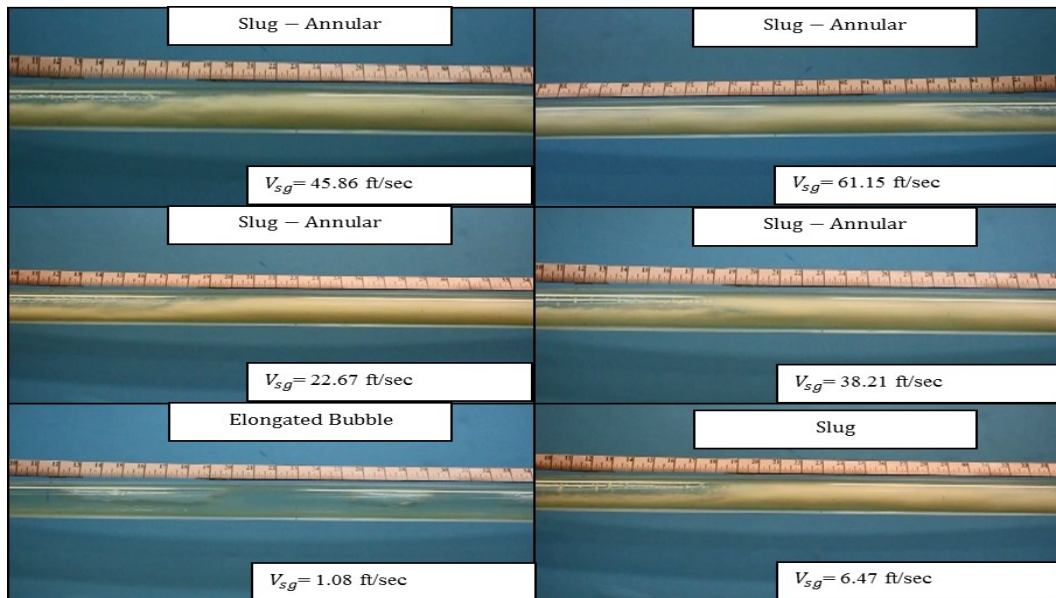


Figure 4.16 Effect of Gas Superficial Velocity of the (Air- 20 Vol % Glycerin Concentration, $V_{SL} = 2.67 \text{ ft/sec}$)

4.1.3.4 Case IV: 30 Vol % Glycerin Concentration ($\mu = 3.10 \text{ cP}$)

In this case, 30 vol % glycerin concentration was added to the water. The viscosity of the solution was 3.10 cP while surface tension and density was 55.4 mN/m, 1 gm/cc

respectively. By comparing this case with the 0.05 vol % surfactant concentration case which has same surface tension value, it is clearly seen in Figure 4.17 that more annular and slug-annular flow regimes were observed and the boundaries between annular/slug-annular and slug-annular/slug shifted down due to increase in viscosity. The effect of increasing gas superficial velocity at fixed liquid superficial velocity ($V_{SL} = 2.67$ ft/sec) is shown in Figure 4.18.

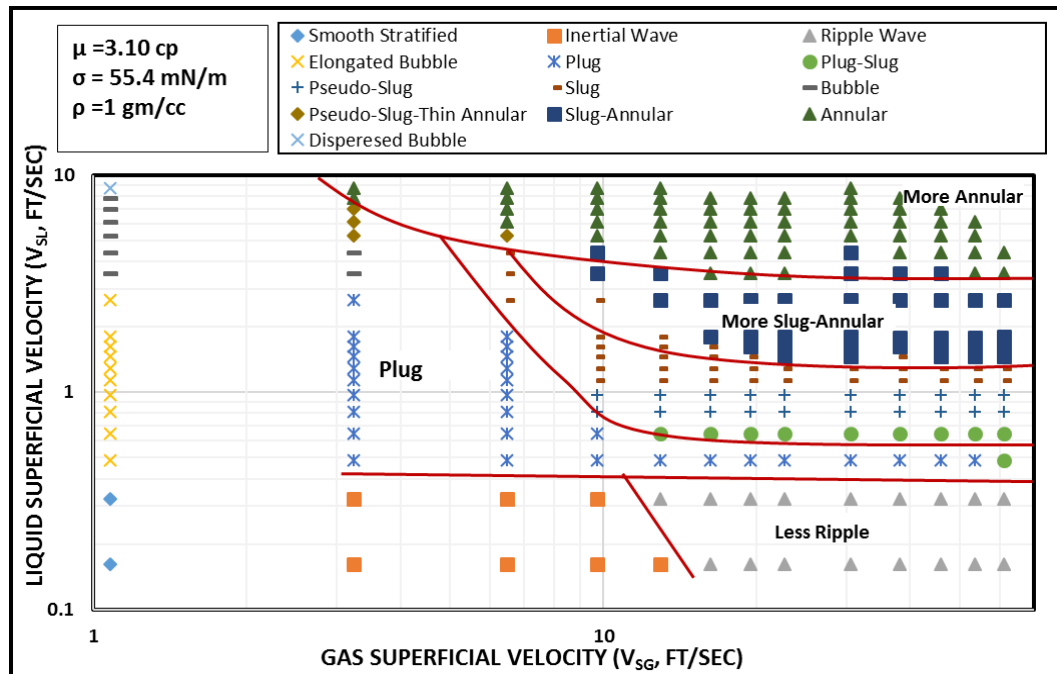


Figure 4.17 Flow Pattern Map of the (Air- 30 Vol % Glycerin Concentration)

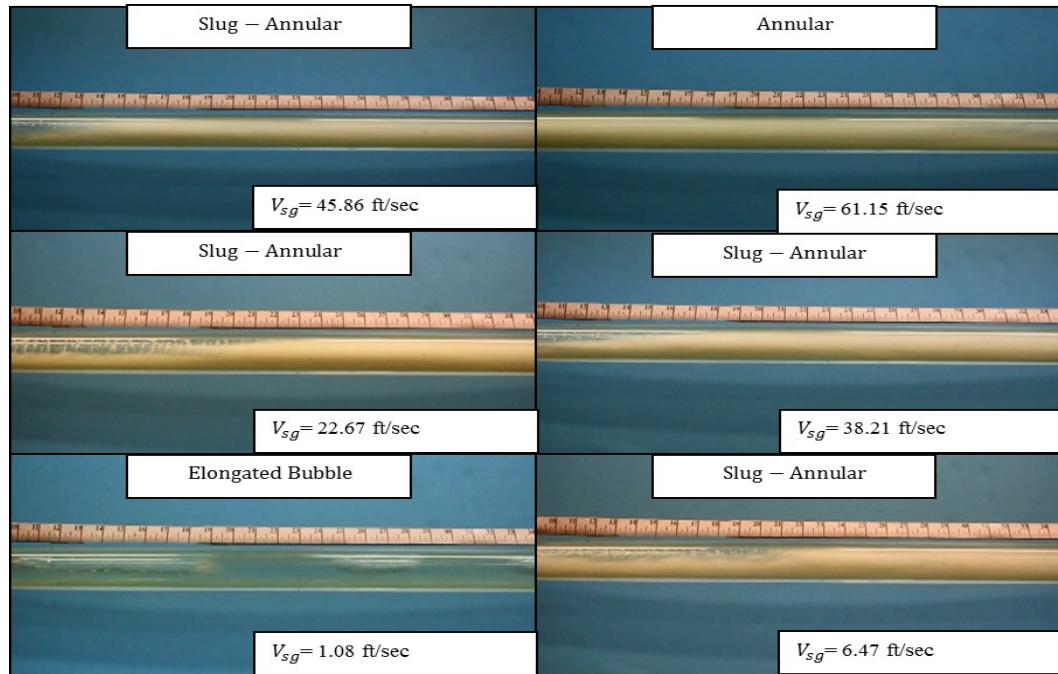


Figure 4.18 Effect of Gas Superficial Velocity of the (Air- 30 Vol % Glycerin Concentration, VSL= 2.67 ft/sec)

4.1.4 Effect of Density (ρ)

4.1.4.1 Case I: 25 Vol % CaBr₂-0.004 Vol % Surfactant Concentration ($\rho = 1.2$ gm/cc)

In this case 25 vol % of CaBr₂ with 0.004 vol % of Surfactant were added to the water. The density of the solution was 1.2 gm/cc while surface tension and viscosity were 61.6 mN/m and 1.44 cP respectively. By comparing this case with the 10 vol% glycerin concentration case which in the same range of surface tension and viscosity values, it is clearly seen in Figure 4.19 that more inertial waves and less ripple waves were observed and the boundary between inertial wave/ripple wave shifted to the right due to increase in density. In addition, more annular flow was observed and the boundary between annular flow /slug-annular and slug-annular/ slug flow shifted to the down. The effect of increasing gas superficial velocity at fixed liquid superficial velocity ($V_{SL} = 2.67$ ft/sec) is shown in Figure 4.20.

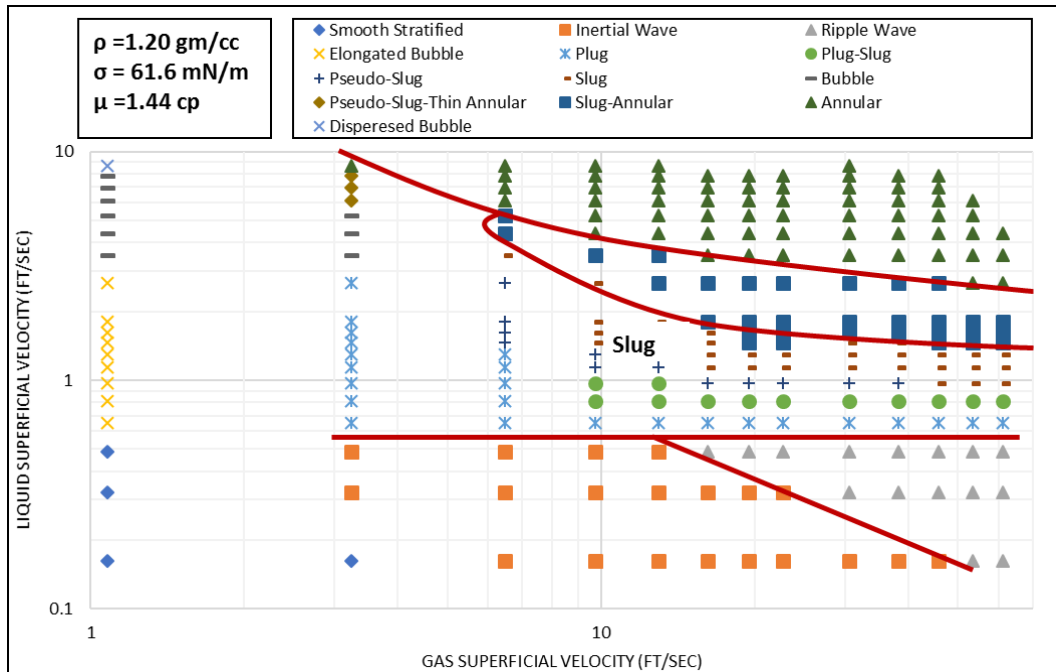


Figure 4.19 Flow Pattern Map of the (Air- 25 Vol% CaBr2-0.004 Vol % Surfactant Concentration)

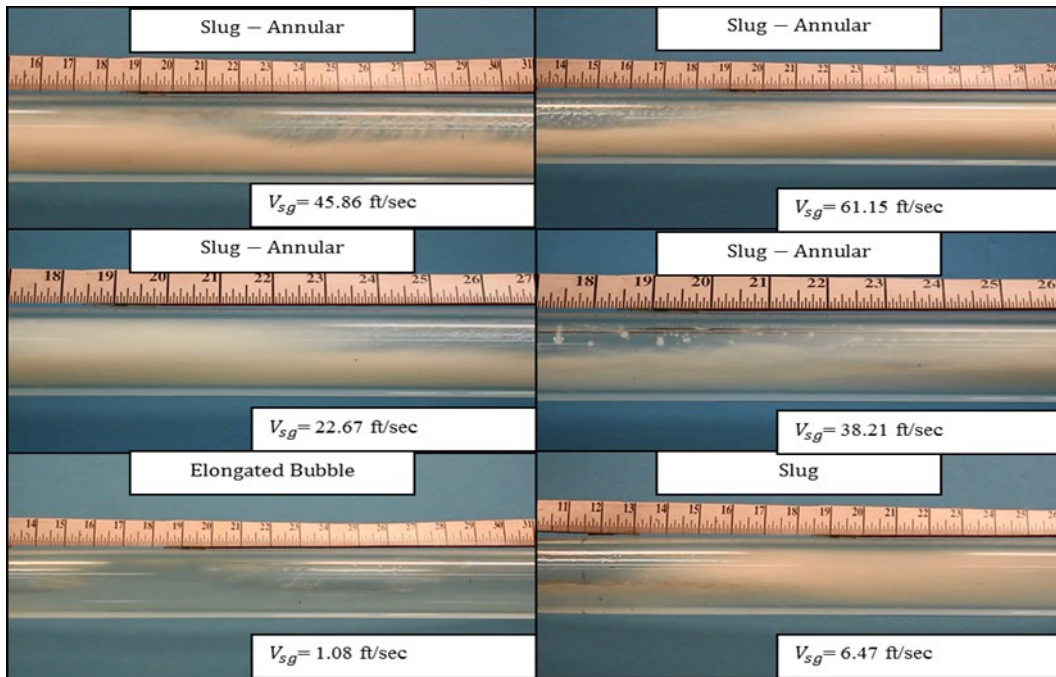


Figure 4.20 Effect of Gas Superficial Velocity of the (Air- 25 Vol % CaBr2-0.004 Vol % Surfactant Concentration, $V_{SL} = 2.67 \text{ ft/sec}$)

4.1.4.2 Case II: 75 Vol % CaBr₂-0.02 Vol % Surfactant Concentration ($\rho = 1.2 \text{ gm/cc}$)

In this case 75 vol % CaBr₂-0.02 vol % Surfactant concentration was added to the water. The density of the solution was 1.5 gm/cc while surface tension and viscosity were 56.3 mN/m, 2.95 cP respectively. By comparing this case with the 30 vol % glycerin concentration case which has same surface tension and viscosity values, it is clearly seen in Figure 4.21 that more inertial waves and more ripple waves were observed and the boundary between inertial wave/ripple wave shifted to the right and the boundary between inertial wave and ripple wave/plug flow shifted up due to increase in density. The effect of increasing gas superficial velocity at fixed liquid superficial velocity ($V_{SL} = 2.67 \text{ ft/sec}$) is shown in Figure 4.22.

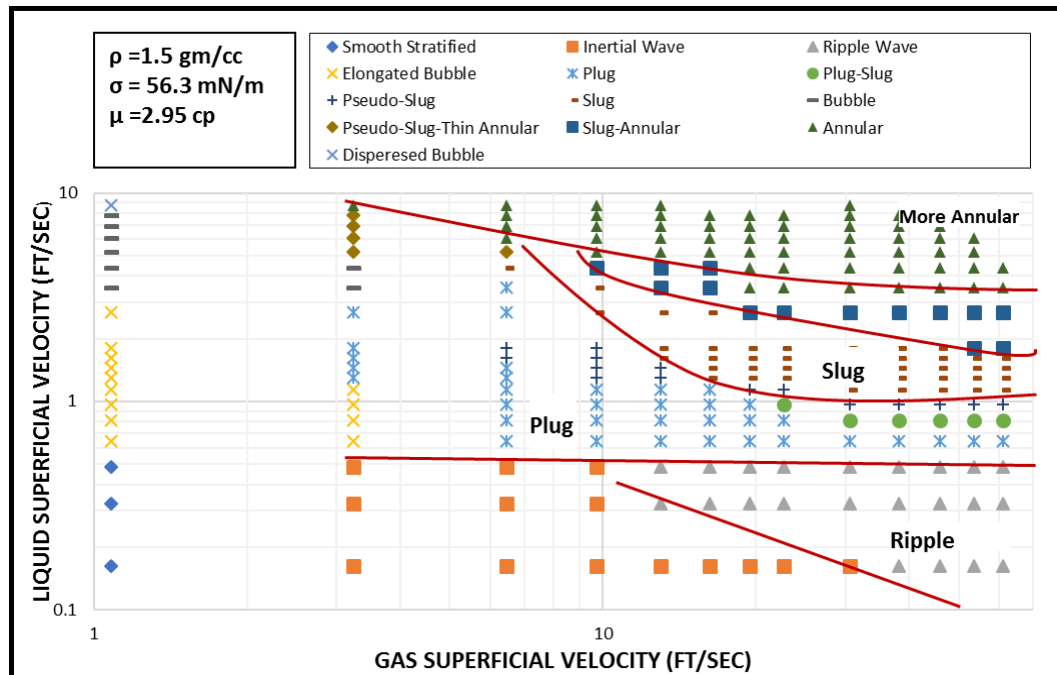


Figure 4.21 Flow Pattern Map of the (Air- 75% Calcium Bromide-0.02% Surfactant Concentration)

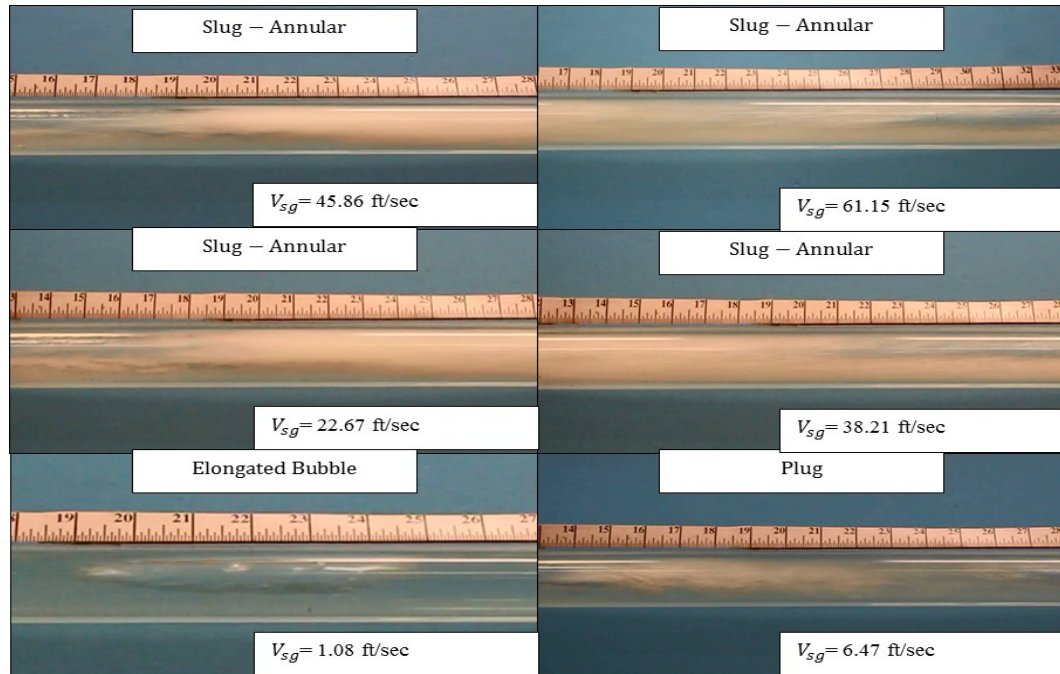


Figure 4.22 Effect of Gas Superficial Velocity of the (Air- 75% CaBr₂-0.02% Surfactant Concentration, VSL= 2.67 ft/sec)

4.2 Pressure Drop Results

Based on the experimental data of the pressure drop for five systems (air-water, air-0.5 vol % surfactant, air-30 vol % glycerin, air- 25 vol %-0.004 vol % surfactant, and air-75 vol % CaBr₂-0.02 vol % surfactant), Pressure drop maps were developed which show the changing of pressure drop due to changing of fluid properties. Figure 4.23 - Figure 4.27 show the effect of fluid properties on the pressure drop for air-water, air-0.5 vol % surfactant, air-30 vol % glycerin, air- 25 vol % CaBr₂-0.004 vol % surfactant and air-75 vol % CaBr₂-0.02 vol % surfactant systems respectively. It can be seen from the pressure drop profiles, that the density has more effect on the pressure drop compared with surface tension and liquid viscosity, where the pressure drop increased due to increasing of density and ranged from 0 to 4.4 psi and from 0 to 5.2 psi for two different systems with density 1.2 gm/cc and 1.5 gm/cc respectively as shown in Figure 4.26 and Figure 4.27.

While the range of pressure drop due to the increase of the liquid viscosity is ranged from 0 to 4.4 psi as shown in Figure 4.25. The pressure drop due to reduction in the surface tension ranged from 0-3.8 psi as shown in Figure 4.24 which is the same range of pressure drop of the air-water system as shown in Figure 4.23.

The density and viscosity have more effect on flow regimes and pressure drop compared with the surface tension that has an effect on flow regimes but has no effect on pressure drop.

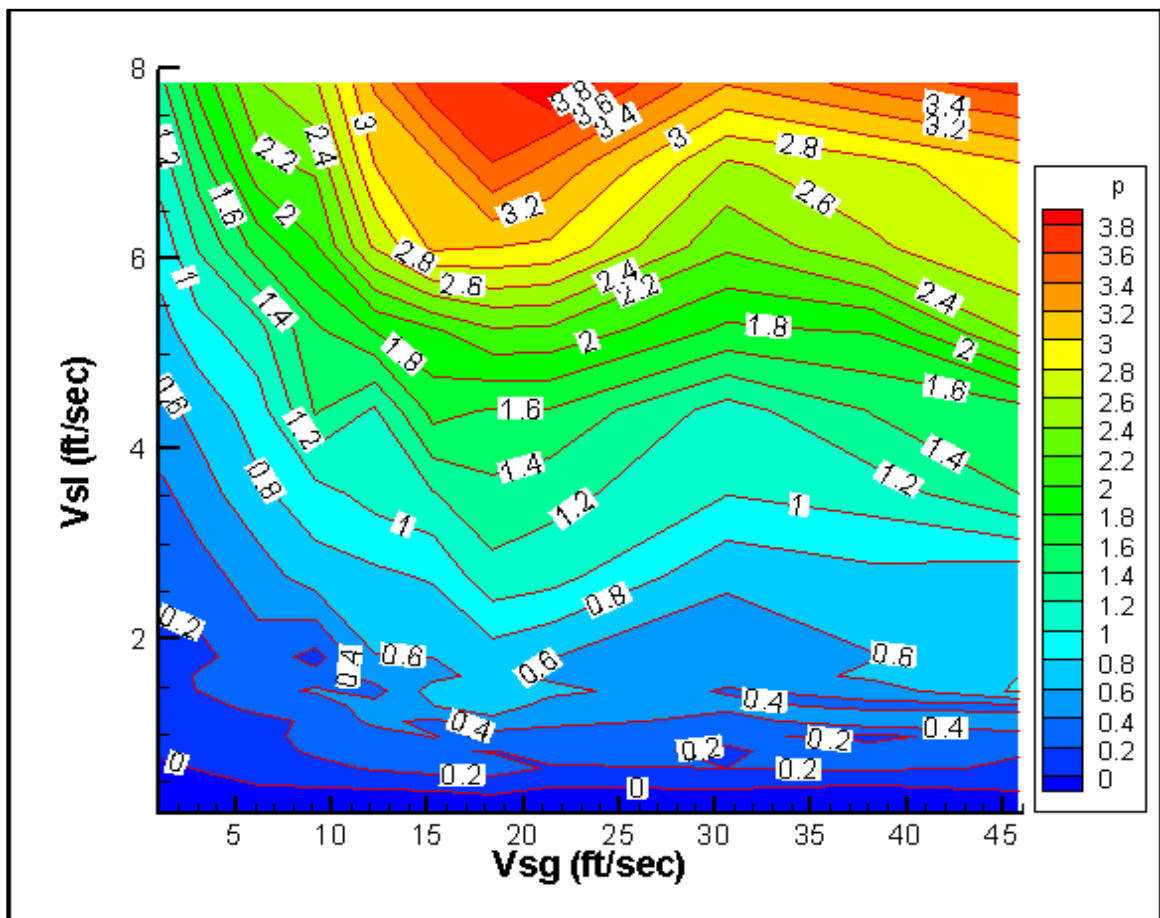


Figure 4.23 Pressure Drop Map of Air-Water System

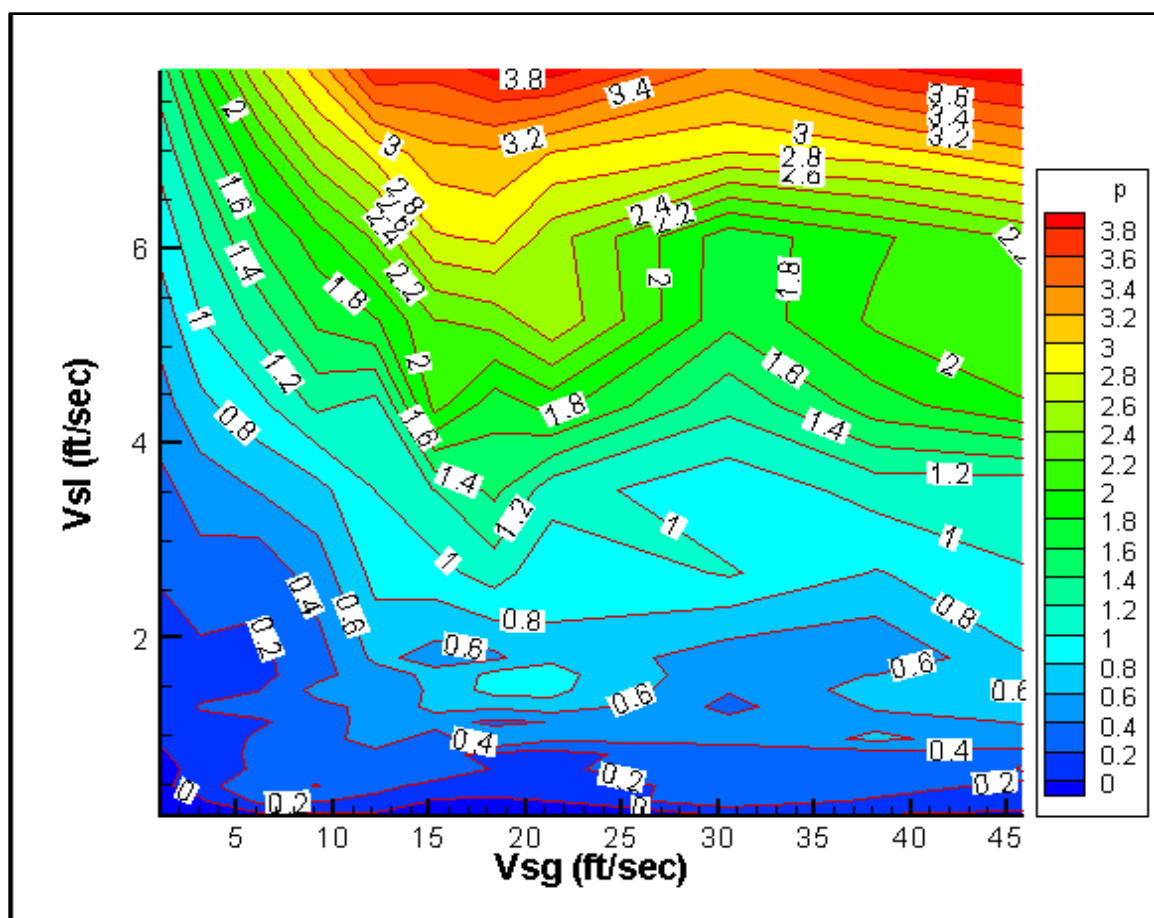


Figure 4.24 Pressure Drop Map of Air-0.05% Surfactant System

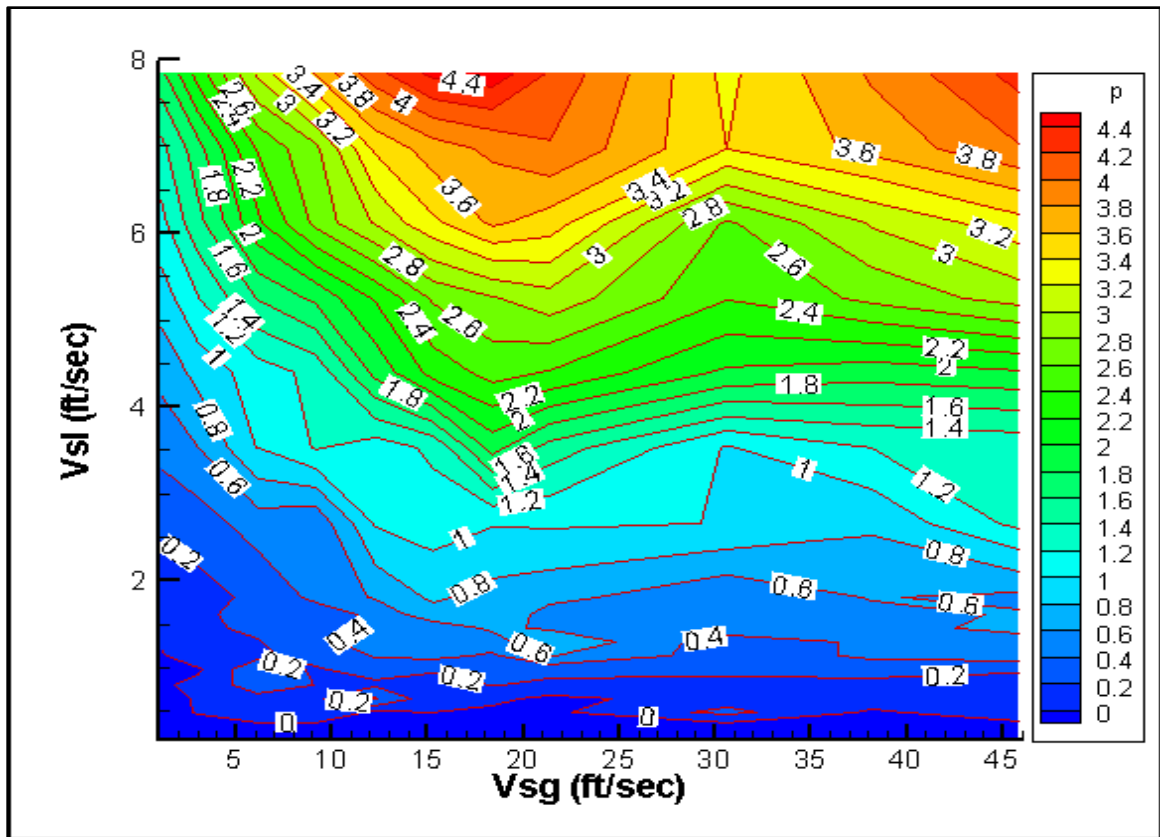


Figure 4.25 Pressure Drop Map of Air-30% Glycerin System

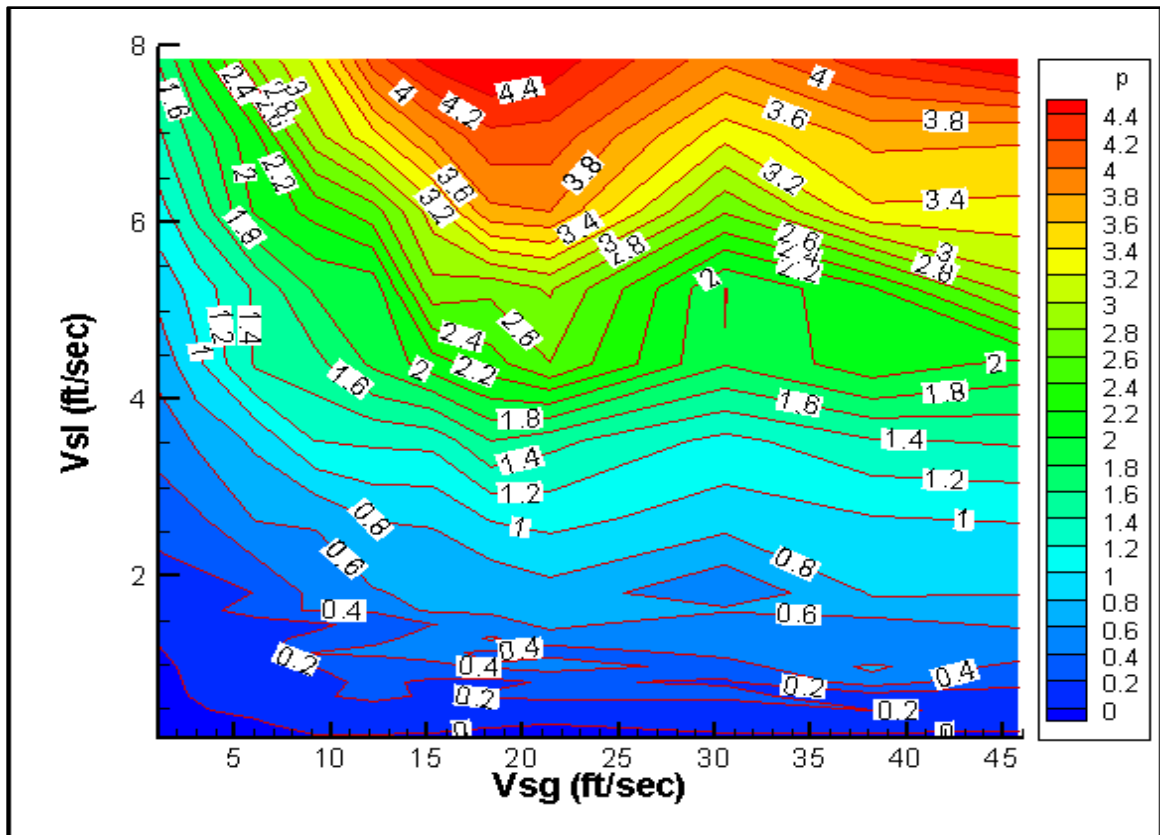


Figure 4.26 Pressure Drop Map of Air-25% CaBr₂-0.004% surfactant System

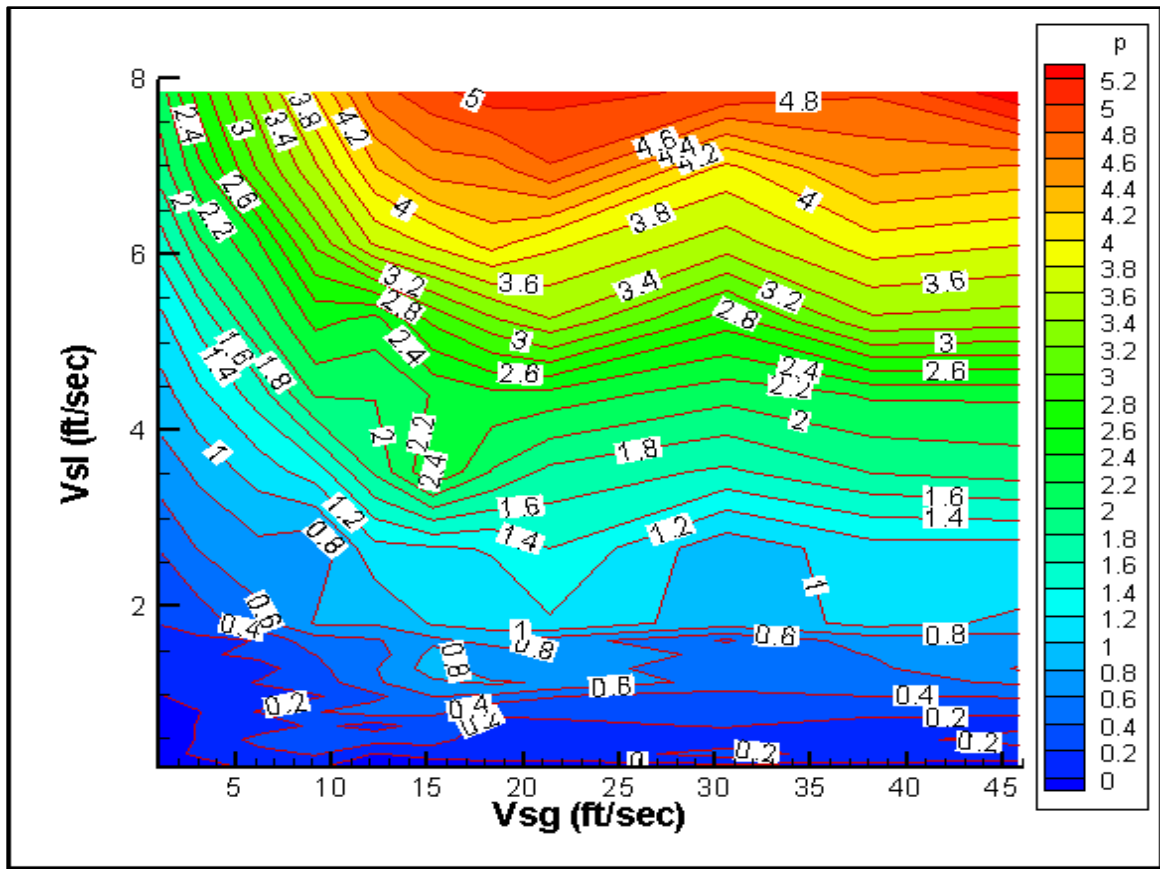


Figure 4.27 Pressure Drop Map of Air-75% CaBr₂-0.02% surfactant System

CHAPTER 5

CONCLUSIONS AND RECOMMENDATIONS

The following conclusions can be made from the effects of density, viscosity and surface tension on flow regimes and pressure drop in horizontal pipes: -

- 1- In general, the changing in density, viscosity and surface tension affect the boundary transition of different flow patterns.
- 2- The density and viscosity have more effect on flow regimes compared with the surface tension effect.
- 3- The effect of viscosity and surface tension on flow regimes is more distinct at a high gas superficial velocity where the boundaries between annular/slug-annular and slug-annular/slug are shifted down due to the reducing of surface tension and increasing of liquid viscosity.
- 4- The effect of density on flow regimes is more distinct at low liquid superficial velocity, where the boundary between inertial wave/ripple wave is shifted to the right and the boundary between wavy stratified/ plug flow are shifted to the up due to the change of liquid density.
- 5- At low surface tension values (0.1 vol % and 0.5 vol % of surfactant), more ripple waves were observed, and pseudo-slug starts vanishing and slug flow starts

appearing.

- 6- At high viscosity (corresponds 30 vol % of glycerin), more annular flow can be seen and the boundaries between annular/slug-annular and slug-annular/slug shifted down due to increase in viscosity.
- 7- At high viscosity, the small effect of hysteresis can be seen at high liquid and gas superficial velocities and there is no effect of hysteresis due to surface tension effect.
- 8- The density and viscosity have more effect on flow regimes and pressure drop compared with the surface tension that has an effect on flow regimes without effect on pressure drop.

The following recommendations can be made as a complement of this work: -

- 1- Developing models considering the effect of fluid properties.
- 2- Study the effect of pressure characteristic of multi-phase flow.
- 3- Evaluate the combined effects of fluid properties and inclination on flow regimes.
- 4- Evaluate the effect of pressure and temperature on multi-phase flow.
- 5- Developing methods to delineate flow regimes.

References

- [1] O. C. J. Jones and N. Zuber, "Statistical methods for measurement and analysis in two-phase flow." Heat transfer, 1974.
- [2] D. Barnea, "A unified model for predicting transitions for the whole range of pipe inclinations," International Journal of Multiphase Flow, vol. 13, no. 1, pp. 1–12, 1987.
- [3] P. L. Spedding and V. A. N. T. Nguyen, "Regime maps for air water two phase flow," Chemical Engineering Science, vol. 35, pp. 779–793, 1979.
- [4] S. L. Kokal and J. F. Stanislav, "An Experimental study of two-phase flow in slightly inclined pipes-I. Flow patterns," Chemical Engineering Science, 1989.
- [5] T. Wong and Y. K. Yau, "Flow patterns in two-phase air-water flow," *Int. Commun. heat mass Transf.*, vol. 24, no. 1, pp. 111–118, 1997.
- [6] M. L. Lamari, "An Experimental investigation of two-phase (air-water) flow regimes in horizontal tube at near atmospheric conditions," Carleton University 2001.
- [7] O. Bergelin and C. Gazley, "Cocurrent gas-liquid flow. I. Flow in Horizontal tubes," Heat Transfer and Fluid Mechanics Institute, Berkeley, California (published by ASME), pp. 5-18, 1949.
- [8] "H.A. Johnson, A.H. Abou-Sabe, "Heat transfer and pressure drop for turbulent flow of air-water mixtures in horizontal pipe," Trans. ASME, 74(6), 977-984, 1952.
- [9] G. Alves, "Cocurrent liquid-gas flow in a pipe-line contactor," *Chem. Eng. Prog.*, 1954.
- [10] O. Baker, "Design of Pipelines for Simultaneous Flow of Oil and Gas," Oil and Gas Journal, July, 26(5) 185-195, 1954.
- [11] D. S. Scott, "Properties of cocurrent gas-liquid flow," Advances in chemical engineering, pp. 199–277, 1964.
- [12] C. Hoogendoorn, "Gas/liquid flow in horizontal pipes," *Chem. Eng. Sc.*, vol. 9, pp. 205–216, 1959.
- [13] G. Govier and M. Omer, "The horizontal pipeline flow of air-water mixtures," *Can. J. Chem.*, 1962.
- [14] K. J. Bell, J. Taborek, and F. Fenoglio, "Interpretation of horizontal in-tube condensation heat transfer correlations with a two-phase flow regime map," *Chem. Eng. Progr., Symp. Ser.*, vol. 66, no. 102, pp. 150–163, 1970.

- [15] P. Whalley, "Boiling, condensation, and gas-liquid flow," 1987.
- [16] B. A. Eaton, C. R. Knowles, I. H. Silberberg, and others, "The prediction of flow patterns, liquid holdup and pressure losses occurring during continuous two-phase flow in horizontal pipelines," *J. Pet. Technol.*, vol. 19, no. 6, pp. 815–828, 1967.
- [17] J. M. Mandhane, G. A. Gregory and K. Aziz "A flow pattern map for gas-liquid flow in horizontal pipes," *International Journal of Multiphase Flow* vol. 1, pp. 537–553, 1974.
- [18] Y. Taitel and A. E. Dukler, "A model for predicting flow regime transitions in horizontal and near horizontal gas-liquid flow," *AIChE J.*, vol. 22, no. 1, pp. 47–55, Jan. 1976.
- [19] J. Weisman, D. Duncan, J. Gibson, and T. Crawford, "Effects of fluid properties and pipe diameter on two-phase flow patterns in horizontal lines," *Int. J. Multiph. Flow*, vol. 5, no. 6, pp. 437–462, Dec. 1979.
- [20] W. Choe and L. Weinberg, "Observation and correlation of flow pattern transitions in horizontal cocurrent gas-liquid flow," *Two-Phase Transp.*, 1976.
- [21] D. Barnea, O. Shoham, Y. Taitel, and A. E. Dukler, "Flow pattern transition for gas-liquid flow in horizontal and inclined pipes. Comparison of experimental data with theory," *Int. J. Multiph. Flow*, vol. 6, no. 3, pp. 217–225, Jun. 1980.
- [22] D. Barnea, Y. Luninski, and Y. Taitel, "Flow pattern in horizontal and vertical two-phase flow in small Diameter Pipes," *Can. J. Chem. Eng.*, vol. 61, no. 5, pp. 617–620, 1983.
- [23] P. Y. Lin and T. J. Hanratty, "Effect of pipe diameter on flow patterns for air-water flow in horizontal pipes," *International journal of multiphase flow*, vol. 13, no. 4, pp. 549–563, 1987.
- [24] Z. El-Oun, "Gas-liquid Two-phase Flow in Pipelines," *SPE Annu. Tech. Conf. Exhib.*, 1990.
- [25] P. L. Spedding and D. R. Spence, "Flow regimes in two-phase gas-liquid flow," *Int. J. Multiph. Flow*, vol. 19, no. 2, pp. 245–280, 1993.
- [26] A. H. Lee, J. Y. Sun, and W. P. Jepson, "Study of flow regime transitions of oil water-gas mixtures in horizontal pipelines," 1993.
- [27] N. P. Hand and P. L. Spedding, "Horizontal gas-liquid flow at close to atmospheric conditions," *Chem. Eng. Sci.*, vol. 48, no. 12, pp. 2283–2305, 1993.
- [28] J. W. Coleman and S. Garimella, "Characterization of two-phase flow patterns in small diameter round and rectangular tubes," *Int. J. Heat Mass Transf.*, vol. 42, no. 15, pp. 2869–2881, 1999.
- [29] P. L. Spedding, R. K. Cooper, and W. J. McBride, "A Universal flow regime map

for horizontal two-phase flow in Pipes,” *Dev. Chem. Eng. Miner. Process*, vol. 11, no. 1/2, pp. 95–106, 2003.

- [30] E. Benard and P. L. Spedding, “Stratified roll wave in horizontal-pipe two-phase flow,” *Ind. Eng. Chem. Res.*, vol. 45, no. 10, pp. 3763–3765, 2006.
- [31] B. Gokcal, Q. Wang, H. Zhang, C. Sarica, and U. Tulsa, “SPE 102727 Effects of high oil viscosity on oil / gas flow behavior in horizontal pipes,” 2006.
- [32] L. A. de Oliveira, J. S. Cunha Filho, J. L. H. Faccini, and J. Su, “Visualization of Two-Phase Gas-Liquid Flow Regimes in Horizontal and Slightly-Inclined Circular Tubes,” no. 1974, 2010.
- [33] C. Tzotzi, V. Bontozoglou, N. Andritsos, and M. Vlachogiannis, “Effect of fluid properties on flow Patterns in two-phase gas - liquid flow in horizontal and downward pipes,” *Ind. Eng. Chem. Res.*, 2010.
- [34] A. Ba geri, R. Gajbhiye, and A. Abdulraheem, “SPE-188009-MS Evaluating the effect of surface tension on two-phase flow in horizontal pipes,” 2017.

Vitae

Name :Ala Shafeq Abdullah AL-Dogail

Nationality :Yemeni

Date of Birth :12/17/1987

Email :a77adogil@gmail.com

Address :Seyion, Hadhramout, Yemen

Academic Background :

B. Sc. Petroleum Engineering, August,2012, Hadhramout University.

Master of Science, Petroleum Engineering, May,2018 King Fahd University of
Petroleum and Minerals.

Experince :

Graduate Assistance at Petroleum Engineering Department, Hadhramout

University, Republic of Yemen (December, 2012- July, 2014).

Technical Qualification :

- TECHLOG Formation Evaluation, King Fahd University of Petroleum and Minerals (March, October 2016).
- CMG-IMEX modeling with BUILDER, King Fahd University of Petroleum and Minerals (February 2015).
- Exploration Methods (Geophysics and Geology), Hadhramout University (March 2014).
- Summer Training Program, Assistant Production Engineer, PETRO MASILA company (2012).